

# Oil & Natural Gas Technology

## The Bakken – An Unconventional Petroleum and Reservoir System

### Final Scientific/Technical Report September 18, 2008 – December 31, 2011

Principal Author: Dr. J. Frederick Sarg

Date Issued: March, 2012

**DOE Award No.: DE-NT0005672**

Submitted by:  
Colorado School of Mines  
1516 Illinois St.  
Golden, CO 80401

Prepared for:  
United States Department of Energy  
National Energy Technology Laboratory



**Office of Fossil Energy**

Acknowledgment: "This material is based upon work supported by the Department of Energy under Award Number DE-NT0005672."

Disclaimer: "This report was prepared as an account of work sponsored by an agency of the United States Government. Neither the United States Government nor any agency thereof, nor any of their employees, make any warranty, express or implied, or assumes any legal liability or responsibility for the accuracy, completeness, or usefulness of any information, apparatus, product, or process disclosed, or represents that its use would not infringe privately owned rights. Reference herein to any specific commercial product, process, or service by trade name, trademark, manufacturer, or otherwise does not necessarily constitute or imply its endorsement, recommendation, or favoring by the United States Government or any agency thereof. The views and opinions of authors expressed herein do not necessarily state or reflect those of the United States Government or any agency thereof."

## ABSTRACT

An integrated geologic and geophysical study of the Bakken Petroleum System, in the Williston basin of North Dakota and Montana indicates that: (1) dolomite is needed for good reservoir performance in the Middle Bakken; (2) regional and local fractures play a significant role in enhancing permeability and well production, and it is important to recognize both because local fractures will dominate in on-structure locations; and (3) the organic-rich Bakken shale serves as both a source and reservoir rock.

The Middle Bakken Member of the Bakken Formation is the target for horizontal drilling. The mineralogy across all the Middle Bakken lithofacies is very similar and is dominated by dolomite, calcite, and quartz. This Member is comprised of six lithofacies: (A) muddy lime wackestone, (B) bioturbated, argillaceous, calcareous, very fine-grained siltstone/sandstone, (C) planar to symmetrically ripple to undulose laminated, shaly, very fine-grained siltstone/sandstone, (D) contorted to massive fine-grained sandstone, to low angle, planar cross-laminated sandstone with thin discontinuous shale laminations, (E) finely inter-laminated, bioturbated, dolomitic mudstone and dolomitic siltstone/sandstone to calcitic, whole fossil, dolomitic lime wackestone, and (F) bioturbated, shaly, dolomitic siltstone. Lithofacies B, C, D, and E can all be reservoirs, if quartz and dolomite-rich (facies D) or dolomitized (facies B, C, E). Porosity averages 4-8%, permeability averages 0.001-0.01 mD or less. Dolomitic facies porosity is intercrystalline and tends to be greater than 6%. Permeability may reach values of 0.15 mD or greater. This appears to be a determinant of high productive wells in Elm Coulee, Parshall, and Sanish fields. Lithofacies G is organic-rich, pyritic brown/black mudstone and comprises the Bakken shales. These shales are siliceous, which increases brittleness and enhances fracture potential.

Mechanical properties of the Bakken reveal that the shales have similar effective stress as the Middle Bakken suggesting that the shale will not contain induced fractures, and will contribute hydrocarbons from interconnected micro-fractures. Organic-rich shale impedance increases with a reduction in porosity and an increase in kerogen stiffness during the burial maturation process. Maturation can be directly related to impedance, and should be seismically mappable.

Fractures enhance permeability and production. Regional fractures form an orthogonal set with a dominant NE-SW trend parallel to  $\sigma^1$ , and a less prominent NW-SE trend. Many horizontal wells are drilled perpendicular to the  $\sigma^1$  direction to intersect these fractures. Local structures formed by basement tectonics or salt dissolution generate both hinge parallel and hinge oblique fractures that may overprint and dominate the regional fracture signature. Horizontal micro-fractures formed by oil expulsion in the Bakken shales, and connected and opened by hydro-fracturing provide permeability pathways for oil flow into wells that have been hydro-fractured in the Middle Bakken lithofacies.

Results from the lithofacies, mineral, and fracture analyses of this study were used to construct a dual porosity Petrel geo-model for a portion of the Elm Coulee Field. In this field, dolomitization enhances reservoir porosity and permeability. First year cumulative production helps locate areas of high well productivity and in deriving fracture swarm distribution. A fracture model was developed based on high productivity well distribution, and regional fracture distribution, and was combined with favorable matrix properties to build a dual porosity geo-model.

## TABLE OF CONTENTS

Executive Summary .....	5
Introduction .....	7
Reservoir Character .....	9
Bakken Lithofacies .....	9
Bakken Stratigraphy .....	21
Mineral and Reservoir Quality .....	24
Rock Physics, Anisotropy, and Organic Maturity .....	32
Sub-Regional Structural Analysis .....	37
Integrated Geo-Model at Elm Coulee Field .....	46
Bakken Exploration Model .....	58
Conclusions .....	59
References .....	61
Bibliography .....	63

## EXECUTIVE SUMMARY

The Bakken Petroleum System, in the Williston basin of North Dakota and Montana, is the most important oil resource play in the continental United States, and is estimated to have 3-4 billion barrels of recoverable oil (USGS estimate). This integrated geologic-geophysical study has accomplished five major objectives over the three year project life: (1) characterization of the lithofacies and mineralogy of the Bakken to identify high performing reservoirs, (2) established that the organic-rich Bakken shales have similar elastic properties and effective stress as the Middle Bakken siltstones and sandstones, suggesting that the shales will not contain induced fractures, and will contribute hydrocarbons from interconnected micro-fractures, (3) established criteria for identifying and mapping natural fractures that are both regional and related to local structures, to guide horizontal wells to optimize fracture intersection, (4) constructed a dual-porosity Petrel geo-model for a portion of the Elm Coulee Field to provide a starting model for reservoir simulation, and (5) developed criteria to assess the Bakken exploration potential in undrilled areas of the basin.

The Middle Bakken Member of the Bakken Formation is the target for horizontal drilling. The mineralogy across all the Middle Bakken lithofacies is very similar and is dominated by dolomite, calcite, and quartz. This Member is composed of six lithofacies: (A) muddy lime wackestone, (B) bioturbated, argillaceous, calcareous, very fine-grained siltstone/sandstone, (C) planar to symmetrically ripple to undulose laminated, shaly, very fine-grained siltstone/sandstone, (D) contorted to massive fine-grained sandstone, to low angle, planar cross-laminated sandstone with thin discontinuous shale laminations, (E) finely inter-laminated, bioturbated, dolomitic mudstone and dolomitic siltstone/sandstone and calcitic, whole fossil, dolomitic-to lime wackestone, and (F) bioturbated, shaly, dolomitic siltstone. Lithofacies B, C, D, and E can all be reservoirs, if quartz and dolomite-rich (facies D) or dolomitized (facies B, C, E). Porosity averages 4-8%, permeability averages 0.001-0.01 mD or less. Matrix reservoir quality is enhanced by dolomitization. Porosity is intercrystalline and tends to be greater than 6%. Permeability may reach values of 0.15 mD or greater. This appears to be a determinant of high productive wells in Elm Coulee, Parshall, and Sanish fields. The Bakken shales comprise lithofacies G and are an organic-rich pyritic brown/black mudstone. The Bakken shales are siliceous, which increases brittleness and enhances fracturing potential.

Analysis of the mechanical properties of the Bakken Formation has contributed to two areas of uncertainty in this resource play. A significant area of controversy in the Bakken resource play is what role the organic-rich shales play in containing fractures and contributing oil to production. Mechanical properties measured in this study, reveal that the Bakken shales probably have similar elastic properties and effective stress values as the Middle Bakken carbonate-rich siltstones and sandstones, and limestones suggesting that the shale will not contain induced fractures. Importantly, horizontal micro-fractures formed by oil expulsion in these shales, connected and opened by hydro-fracturing, will provide permeability pathways for oil flow into wells that have been hydro-fractured in the Middle Bakken lithofacies, and will contribute hydrocarbons to well production. Secondly, predicting the mature to immature transitions within the Bakken can help identify trap potential, but has a measure of uncertainty. Work in this study shows that the impedance of these organic-rich shales increases with a reduction in porosity and an increase in

kerogen stiffness during the burial maturation process. The degree of maturation can thus be directly related to impedance and should be a seismically mappable parameter.

Fractures enhance permeability and production and are both regional and local in distribution. Regional fractures form an orthogonal set with a dominant NE60SW trend parallel to  $\sigma^1$ , and a less prominent NW150SE trend. Many horizontal wells are drilled perpendicular to the  $\sigma^1$  direction to intersect these fractures. Local structures formed by basement tectonics or salt dissolution generate both hinge parallel and hinge oblique fractures that may overprint and dominate the regional fracture signature. This project has demonstrated that differentiating and mapping these different fracture systems can be done using seismic attributes such as minimum curvature. This should help optimize planning of horizontal well azimuths.

Results from the above lithofacies, mineralogical, mechanical property, and fracture analyses of this integrated study were used to construct a dual porosity Petrel geo-model for a portion of the Elm Coulee Field. In Elm Coulee, dolomitization enhances reservoir porosity and permeability. First year cumulative production was the key factor in locating areas of high well productivity and in deriving fracture swarm distribution. A fracture model was developed based on high productivity well distribution, and regional fracture distribution, and was combined with favorable matrix properties to build a dual porosity geo-model.

Parameters and criteria have been developed to identify areas where new traps may be found, and where enhanced productivity of Bakken oil is possible. The criteria are grouped into four categories – (1) source and maturation, (2) reservoir quality of matrix, (3) natural fractures, and (4) trap and seal.

1. The Bakken shales are mature over much of the basin, and are still generating oil. Large fields (Elm Coulee, Sanish, and Parshall) are located at the transition from mature to immature level of maturation. Volume increases during maturation by as much as 30% provide necessary overpressure to allow highly productive wells. Volume decrease at the transition to immature source rock is important to providing updip seal.
2. Reservoirs are present both in the Middle Bakken and the Upper Bakken Shale. Middle Bakken lithofacies can all be reservoirs, if quartz-rich and/or dolomitized. Porosity averages 4-8%, permeability averages 0.01-0.001 mD or less. Reservoir quality is enhanced by dolomitization. Porosity is intercrystalline and tends to be greater than 6%. Permeabilities may reach to 0.15 mD or greater. The Bakken shales are siliceous, increasing brittleness and enhancing hydro-fracturing potential. During oil generation, volume increase causes overpressure (0.6 - 0.73 psi/ft pressure gradient) and horizontal micro-fractures in the shale enhance permeability.
3. Regional fractures and faults form an orthogonal set with a dominant NE-SW direction parallel to  $\sigma^1$ ). Local structures form both hinge parallel and hinge oblique fractures that may overprint and dominate the fracture signature.
4. Although the Bakken is a basinwide resource play, large accumulations do appear to have significant trap and seal components. Traps include (1) hydrodynamic traps at the mature to immature boundary (e.g., Parshall field, North Dakota); 2) stratigraphic pinch out of the Middle Bakken (e.g., Elm Coulee field, Montana); 3) porosity pinch out of Middle Bakken dolomitic facies (e.g., Elm Coulee field, Montana), and 4) lateral facies changes in Middle Bakken (e.g., View Field, Canada).

## INTRODUCTION

The Bakken Formation, a Devonian-Mississippian black shale and mixed sandstone/carbonate unit, is an important source rock for oils produced in the Williston Basin (Figure 1). Recent advances in horizontal drilling, fracture stimulation and completion technology have turned this once uneconomical play into commercial reality. The Bakken Petroleum System of the Williston Basin consists of source beds in the Bakken (upper and lower shales) and lower Lodgepole (False Bakken) and reservoirs in the lower Lodgepole (Scallion), middle Bakken silty dolostones, Sanish Sandstone, and upper Three Forks silty dolostones (Figure 2). The source rocks are world class with total organic carbon contents averaging 11 weight percent (Webster, 1984). The reservoirs have been recognized as having low porosity and permeability, regional hydrocarbon charge, and are thought to be fracture enhanced where productive (Murray, 1968; Meissner, 1978; Cramer, 1986, 1991). The petroleum system is an unconventional system because of low porosity and permeability of the reservoirs, and pervasive hydrocarbon saturation. Natural fracturing enhances low porosity and permeability reservoirs of the Bakken petroleum system and results in reservoir “sweet spots.” Hydraulic-fracture stimulation and horizontal drilling greatly improves production from the natural sweet spot areas. The first production from the Bakken petroleum system was from the Antelope Field located on the Antelope asymmetric anticline discovered in 1953 (LeFever, 2005). Occurrence of natural fractures along the northwest trending structure enhanced well production. Wells were completed in the “Sanish sandstone” and silty dolostone beds of the upper Three Forks. The Bakken horizontal play began in Montana with the completion of the first well in 2001 and has now moved into North Dakota. The Bakken petroleum system is a continuous type of accumulation in the deeper parts of the Williston basin (Nordeng, 2009). A continuous accumulation is a hydrocarbon accumulation that has some or all of the following characteristics: pervasive hydrocarbon charge throughout a large area; no well-defined oil- or gas-water contact; diffuse boundaries; commonly abnormally pressured (associated with mature source rocks); a large in place resource volume but a low recovery factor; little water production; geologically controlled sweet spots; reservoirs commonly in close proximity to mature source rocks; reservoirs with very low matrix permeabilities; and water occurring up-dip from hydrocarbons.

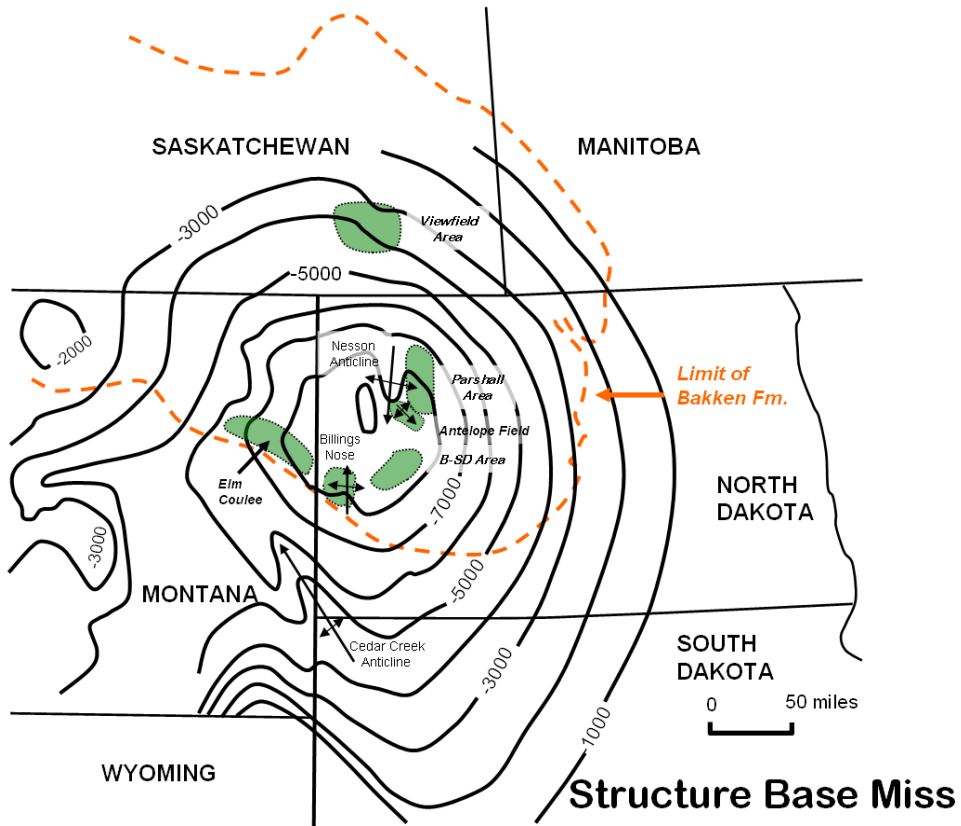


Figure 1. Structure map on the base of the Mississippian. Regional limit of the Bakken Formation is shown by dashed line. Recent Bakken field development areas are shown in green.

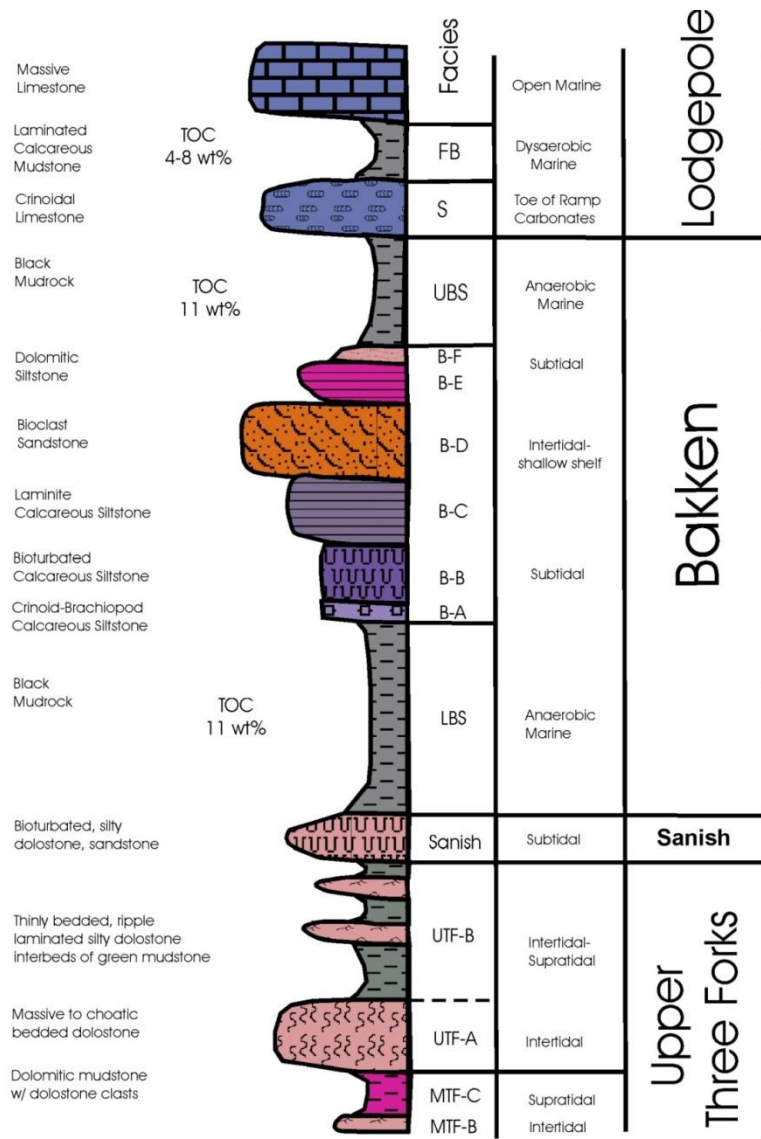


Figure 2. Stratigraphic column for the Bakken petroleum system.

## RESERVOIR CHARACTERIZATION

### Bakken Lithofacies:

Detailed lithofacies of the Bakken Formation provide a framework for the Bakken exploration model and reservoir geo-model (summarized in Figure 1). Descriptions below are based on two field studies completed in Parshall (Simonsen, 2010) and Elm Coulee fields (Alexandre, 2011).

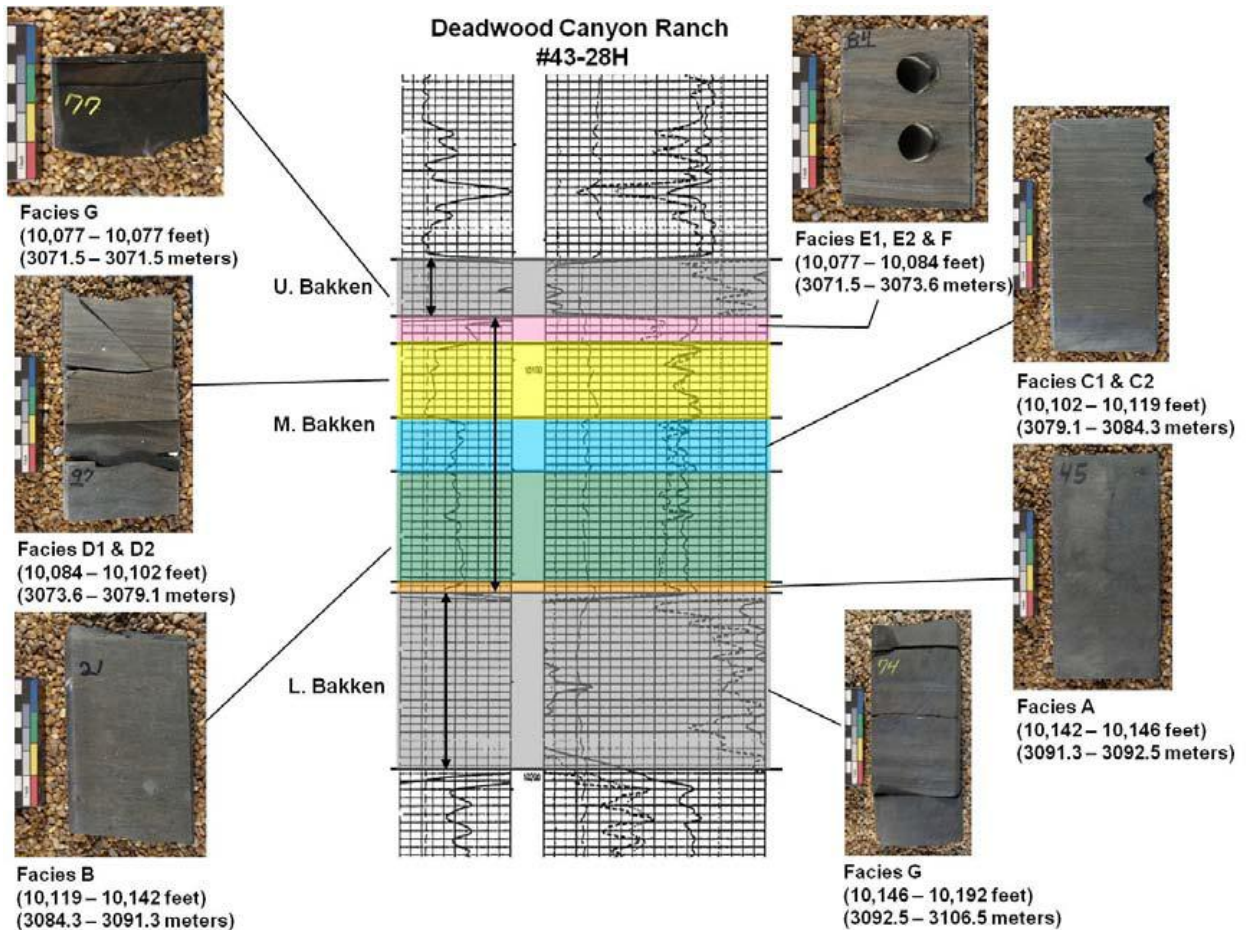


Figure 1. Facies of the Bakken Formation observed from core samples. Facies E is subdivided into E1 and E2, based on sedimentary features, and is combined with facies F for log correlations. Facies D is subdivided into D1 and D2 based on sedimentary structures. Facies C is subdivided into C1 and C2 based on sedimentary structure differences. The log and core pictures were taken from the Deadwood Canyon Ranch #43-28H well (core available by permission from Fidelity Exploration and Production Company).

### **Facies A. Muddy Lime Wackestone**

Facies A consists of a muddy lime wackestone that contains crinoids and brachiopod shell fragments (Figure 2). This thin bed is immediately above the lower Bakken shale and could represent the first influx of carbonates into the system. Porosity is intergranular with calcite and pyrite as the predominant cements. The amount of pyrite increases as the contact with the lower Bakken is approached. This facies ranges in thickness from 1 to 5 feet (0.3 to 1.5 meters), and averages 2.9 feet (0.9 meters), which makes it hard to up by wireline logging tools. When it is thick enough, the gamma ray reading will show a cleaner signal than the overlying B facies. The following core porosity and permeability values come from Parshall Field and are meant to be a representative sample of Middle Bakken values. Core porosity values for this interval range from 2.7% - 6.1% and average 4.5%. The permeability values range from 0.0001 mD – 0.0057 mD (mD = millidarcies) and average 0.0012 mD.



Figure 2. Core photos of facies A – muddy lime wackestone. Crinoid and brachiopod shell fragments are more concentrated at the base of the facies. This lowermost facies of the middle Bakken lies directly above the contact with the lower Bakken shale as seen in photo A.

### **Facies B. Bioturbated, Argillaceous, Calcareous, Very Fine-Grained Siltstone/Sandstone**

Facies B consists of bioturbated, argillaceous, calcareous sandstones and siltstones (Figure 3). Strong bioturbation makes identification of many trace fossils difficult but some common *Helminthopsis/Sclarituba* burrow traces have been identified (Figures 3, 4). Some calcite filled vertical fractures are present and local calcareous concretions are found within this facies. Intergranular and microfracture porosity are present with calcite cement and some pyrite cement. Thickness of this interval ranges from 3 to 34 feet (0.9 to 10.4 meters) and averages 20 feet (6.1 meters). This is the thickest interval in the middle Bakken and is found in all of the cores described. The facies shows up on wireline logs as a thick section of shaly sand. Core porosity values for this interval range from 2.2% - 9.8% and average 5.7%. Permeability values range from 0.0001 mD – 0.03 mD and average 0.0015 mD.

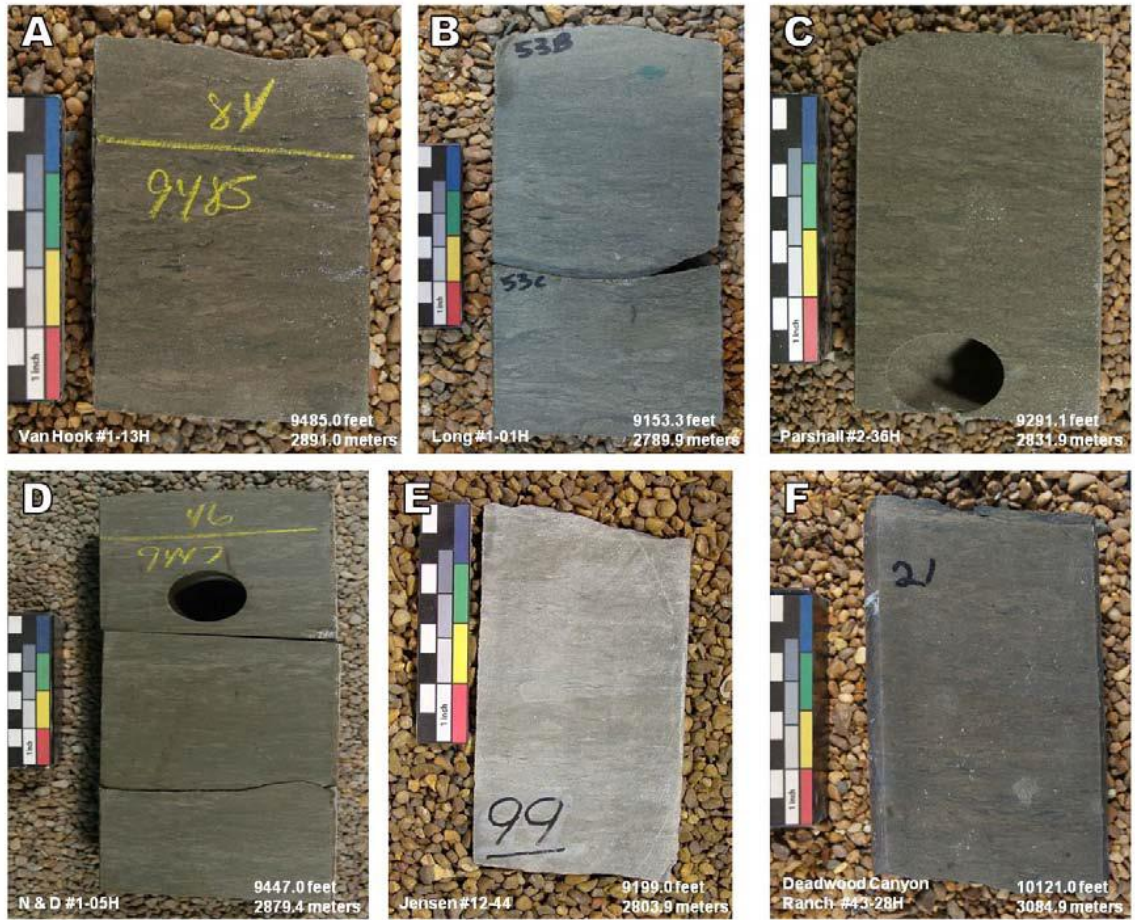


Figure 3. Core photos of facies B – bioturbated, argillaceous, calcareous, silt-stone/sandstone. This is the thickest interval in the Middle Bakken and is present in all of the cores described.

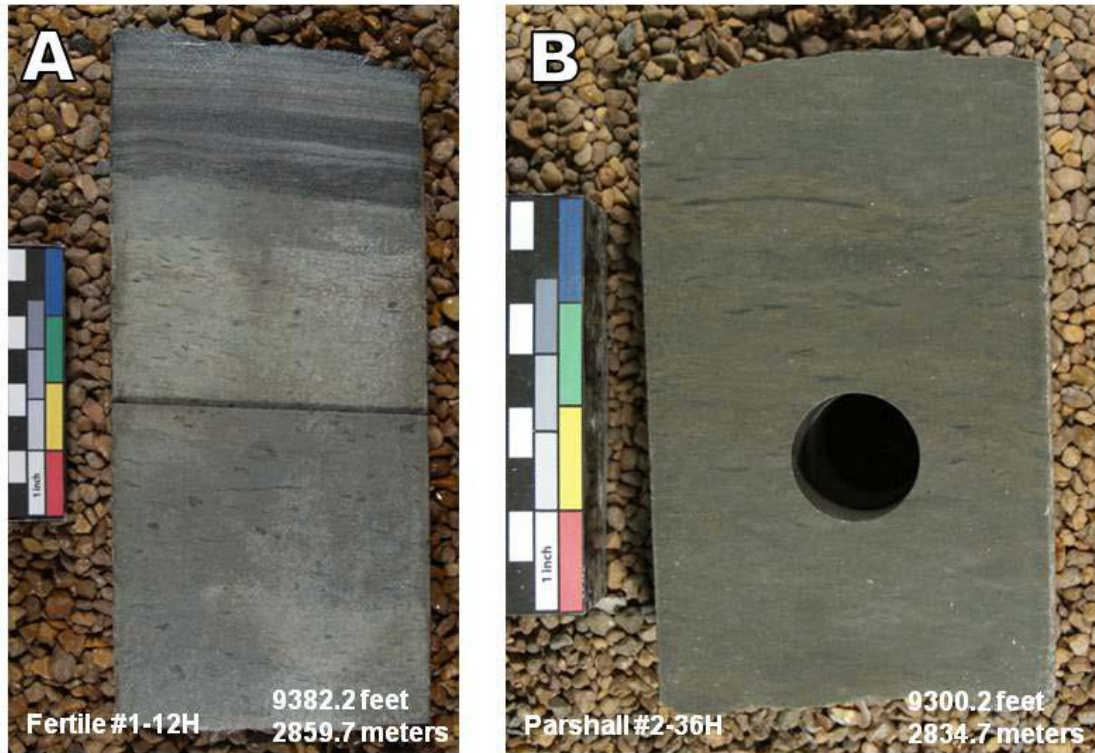


Figure 4. Core photos showing *Helmithopsis/Sclarituba* burrow traces found in facies B.

**Facies C1. Planar to Undulose Laminated, Shaly, Very Fine-Grained Siltstone/Sandstone**

Facies C1 mainly consists of finely laminated shaly sandstone and siltstone. These laminations are on the millimeter and centimeter scale (Figure 5). There are some wavy laminated sections which could possibly be microbial binding of the sediment; however the section is dominated by continuous planar laminations. Intergranular and minimal amounts of intercrystalline porosity are present. On well logs this interval is chosen when the neutron porosity curve and bulk density curve come together with a lowering gamma ray reading. Thickness of this interval ranges from 2 to 14 feet (0.6 to 4.3 meters) with an average of 7.5 feet (2.3 meters). Core porosity values for this interval range from 2.5% - 10.3% and average 6.3%. Permeability values range from 0.0001 mD – 0.01 mD and average 0.0026 mD.

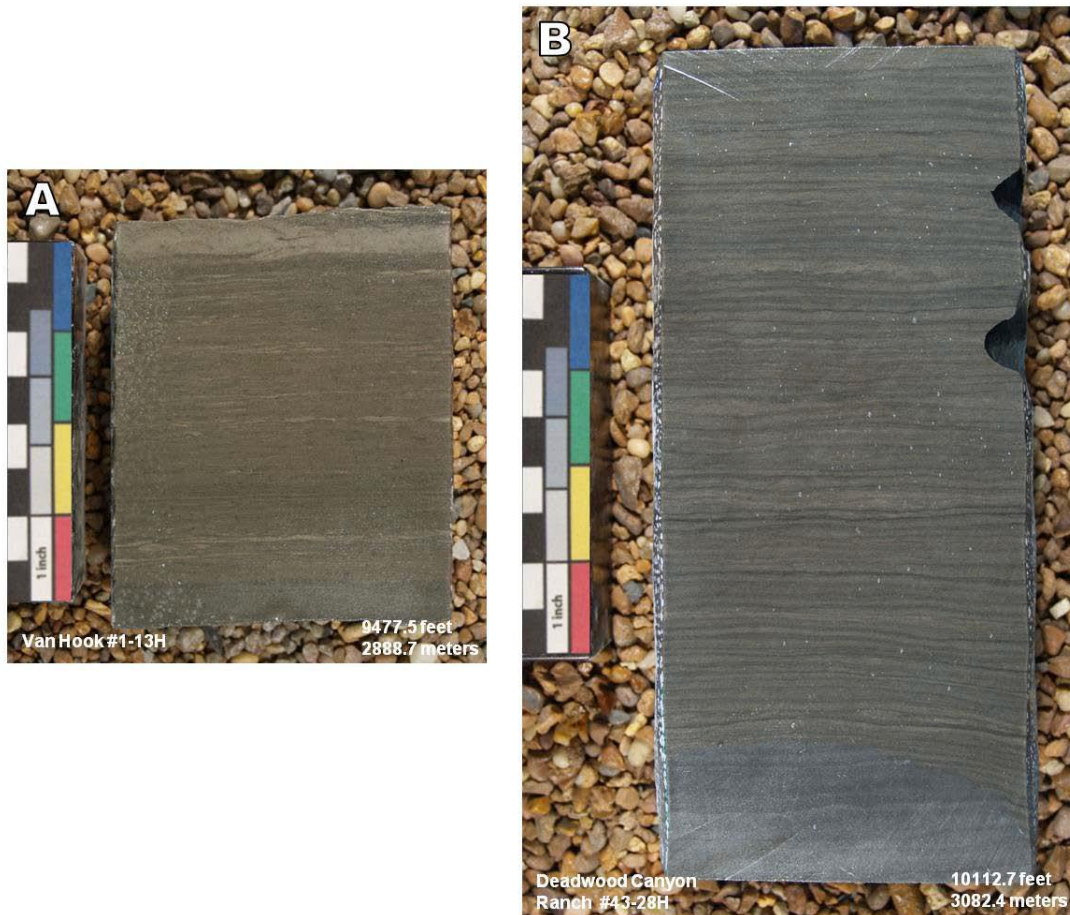


Figure 5. Core photos of facies C1 – planar to undulose laminated, shaly, very fine-grained siltstone/sandstone. This interval is dominated by continuous planar bedding but there also are sections of wavy laminations.

**Facies C2. Symmetrically Ripple to Undulose Laminated, Very Fine-Grained Siltstone/Sandstone**

Facies C2 consists of finely laminated to rippled, shaly, very fine-grained sandstone (Figure 6). Some hummocky cross stratification is present as well as some localized bioturbation. The laminations can look crenulated to irregular and microbial binding of the laminations is present. There is also considerable calcite cement present. Thickness for this interval averages 3 feet (0.9 meters). The thinness of this facies makes it hard to be picked up by wireline logs. Core porosity values for this interval range from 2.3% - 7.5% and average 5.4%. Permeability ranges from 0.0005 mD – 0.027 mD and averages 0.0079 mD.

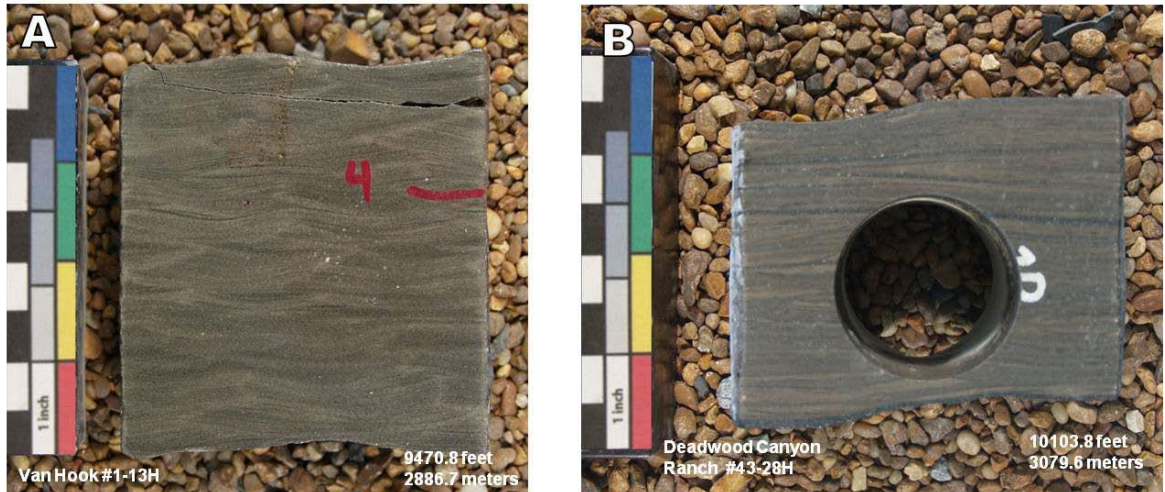


Figure 6. Core photos of facies C2 – symmetrically ripple to undulose laminated, very fine-grained siltstone/sandstone. This facies is only present in two cores described with an average thickness of 3 feet (0.9 meters).

**Facies D1. Contorted to Massive, Fine-Grained Sandstone**

Facies D1 consists of a muddy, contorted to massive, fine-grained sandstone that has common micro-faults, micro-fractures, and slumps representing soft sediment deformation (Figure 7). On well logs, this facies appears just below the cleanest gamma ray readings of facies D2 but is still cleaner than the underlying C2 facies. Thickness of this interval ranges from 2 to 5 feet (0.6 to 1.5 meters). Core porosity values range from 2.0% - 2.6%, averaging 2.3%. Permeability in this facies ranges from 0.0003 mD – 0.0012 mD and average 0.0008 mD.



Figure 7. Core photos of facies D1 – contorted to massive fine-grained sandstone. This facies has common micro-faults, micro-fractures, and slumps representing soft sediment deformation.

**Facies D2. Low Angle, Planar to Slightly Undulose, Cross-Laminated Sandstone with Thin Discontinuous Shale Laminations**

Facies D2 consists of a light brown to light grey, parallel to undulating laminated, low angle cross-laminated sandstone (Figure 8). This facies lacks bioturbation and can be highly cemented by calcite. Some calcite filled fractures are also present. Intergranular porosity is abundant with calcite as the dominant cement. Thickness of the interval ranges from 0 to 22 feet (0.0 to 6.7 meters) and averages 8 feet (2.4 meters) where present. This facies has the cleanest signature on the gamma ray reading from wireline logs (it has been called the “clean bench”). Core porosity values range from 2.5% - 12.8%, averaging 4.3%, and permeability ranges from 0.0001 mD – 0.055 mD, averaging 0.0042 mD.

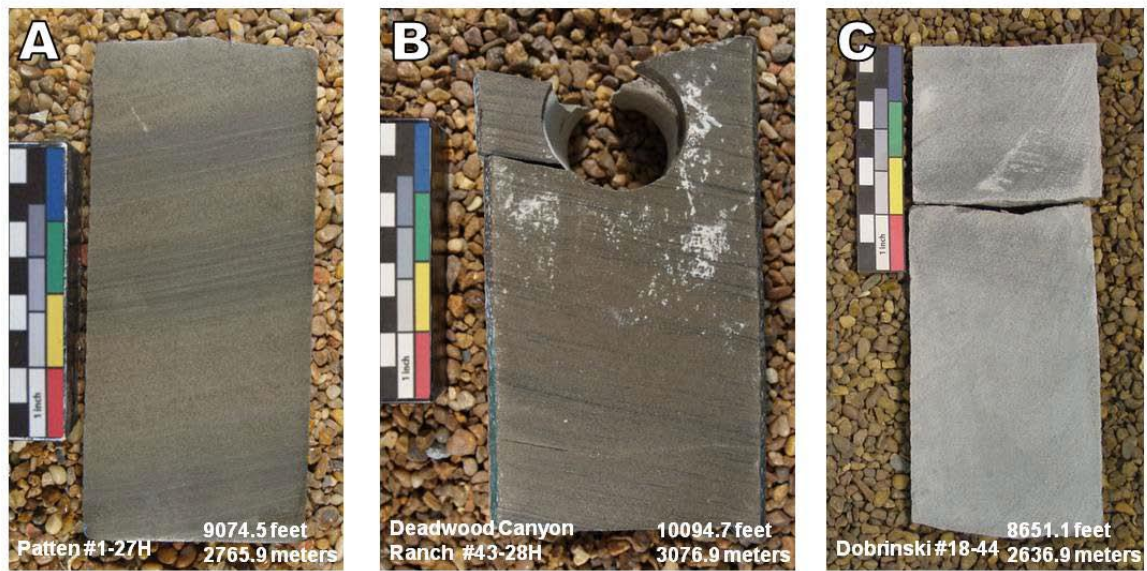


Figure 8. Core photos of facies D2 – low angle, planar to slightly undulose, cross-laminated sandstone with thin discontinuous shale laminations. Photo C shows the more massive limestone unit found in the Dobrinski #18-44 core east of Parshall Field.

**Facies E1. Finely Inter-Laminated, Bioturbated, Dolomitic-Mudstone and Dolomitic Siltstone/Sandstone**

Facies E consists of an interbedded dark grey, highly bioturbated siltstone, and light gray, very fine grained, thin parallel laminated sandstone (Figure 9). Locally strong and moderate bioturbation is present. Thickness of the interval ranges from 5 to 11 feet (1.5 to 3.4 meters), and averages 7.5 feet (2.3 meters). At the base of this facies there is a thin organic-rich mudstone which can be clearly seen on the gamma ray log. Core porosity ranges from 0.5% - 11.3% with an average of 5.7% for this facies. Permeability values range from 0.0001 mD – 0.083 mD with an average permeability of 0.0062 mD. This interval is the most dolomitic zone of the Bakken and is one of the main targets for drilling.

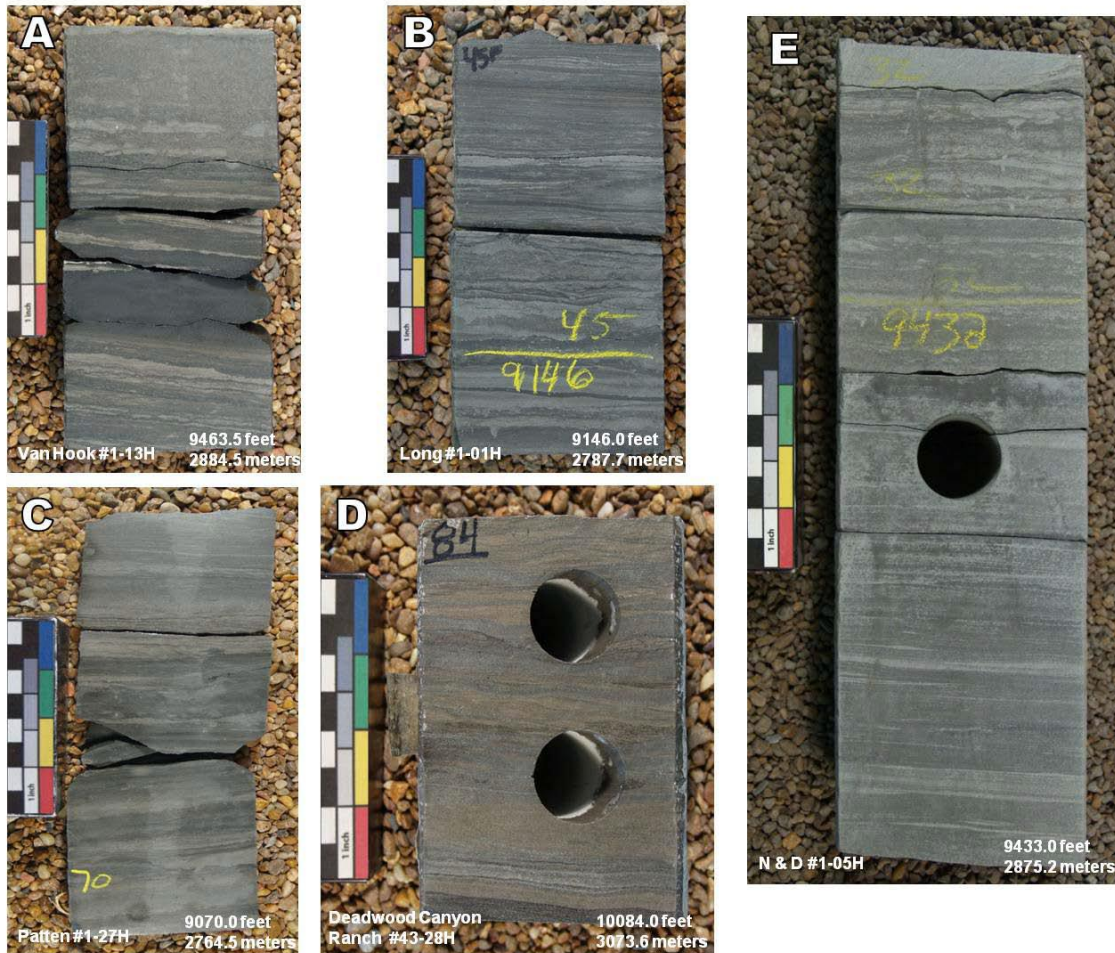


Figure 9. Core photos of facies E1 – finely inter-laminated, bioturbated, dolomitic mudstone and dolomitic siltstone/sandstone.

**Facies E2. Calcitic, Whole Fossil, Dolomitic-to Lime Wackestone**

Facies E2 consists of a calcitic, whole fossil, dolomitic-to lime wackestone with fossil-rich beds (Figure 10). These fossil-rich beds contain crinoid fragments and brachiopods found as articulated shells, single valves, or shell fragments. This facies can be interspersed with facies E1. Thickness of the interval averages only a couple of inches. Only one sample in this facies had core data showing a porosity of 3.3% and permeability of 0.0308 mD. This facies is not well detected on wireline logs due to the thin beds.

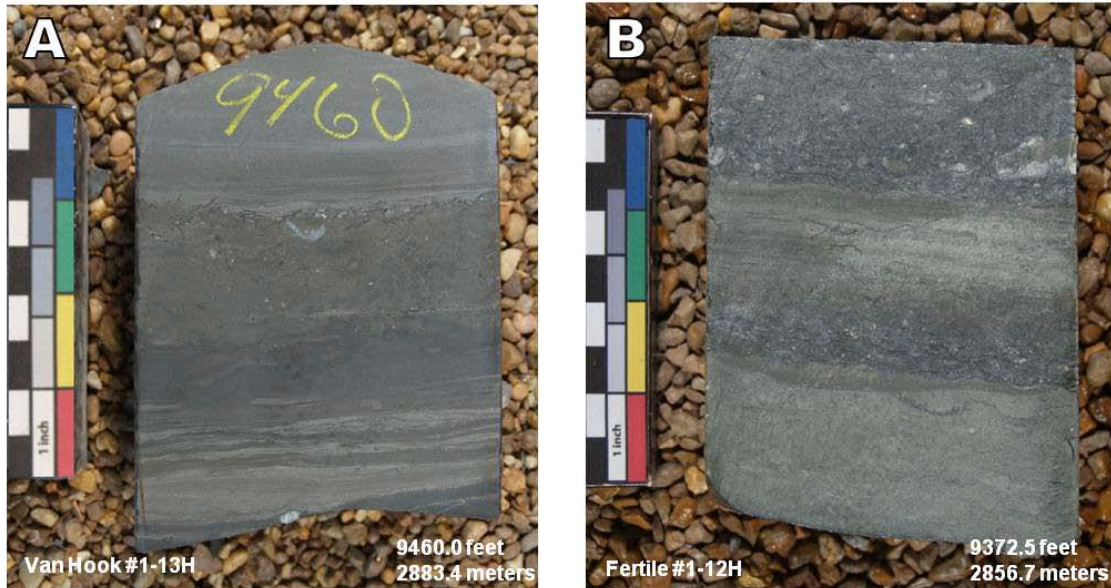


Figure 10. Core photos of facies E2 – calcitic, whole fossil, dolomitic-to lime wackestone. These fossil-rich beds contain brachiopod shells and crinoid fragments and may represent storm deposits.

#### **Facies F. Bioturbated, Shaly, Dolomitic Siltstone**

Facies F consists of a bioturbated, shaly, dolomitic siltstone that lies immediately below the contact with the upper Bakken shale (Figure 11). Little structure is seen within the facies and pyrite gives it a lighter yellow, mottled look. This facies is not present in all of the cores. Thickness of the interval ranges from 2 inches to 3 feet (0.05 to 0.9 meters), averaging 1.5 feet (0.5 meters). This facies is hard to see on wireline logs because of its proximity to the highly radioactive overlying shale that overshadow the signal. Core porosity and permeability in this interval are low due to closely packed dolomite crystals. Porosity in this facies ranges from 4.0% - 7.6% with an average of 6.0%. Permeability is very low measured, ranging from 0.0005 mD – 0.075 mD with an average of 0.0482 mD.

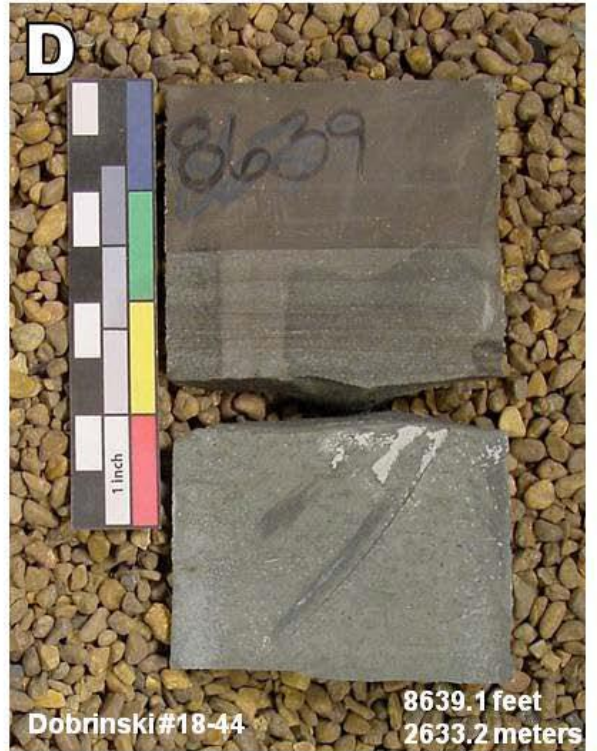


Figure 11. Core photos of facies F – bioturbated, shaly, dolomitic siltstone. This uppermost facies of the middle Bakken lies directly below the contact with the upper Bakken shale as seen in photos C and D.

### Facies G. Organic Rich Pyritic Brown/Black Mudstone

Facies G is characterized by dark gray, brownish-black to black, fissile, non-calcareous, carbonaceous, and bituminous shale (Figure 12). This mudstone interval contains silt-size dolomites, calcites, and quartz. Pyrite is generally disseminated throughout the shale, but also occurs in laminations. This facies also contains calcitic fossil fragments which are difficult to identify. This facies composes both the Upper and Lower Bakken shales.



Figure 12. Core photos of facies G – organic rich pyritic brown/black mudstone. Photos A and B are from the Upper Bakken Shale, and photos C and D are from the Lower Bakken Shale. Small vertical fractures cemented by calcite and pyrite are visible in photo C.

### Bakken Stratigraphy:

The stratigraphic framework includes a compilation of subsurface and surface outcrop data, and stratigraphic interpretation using wells and 3-D seismic contributed by industry participants (Vickery, 2011, Sonnenberg et al., 2011). Biostratigraphic data has been compiled and provides regional correlation for the Williston basin into western Montana and Canada (Figure 13). This framework provides critical data for mapping lateral and vertical heterogeneity in the Bakken sedimentary system.

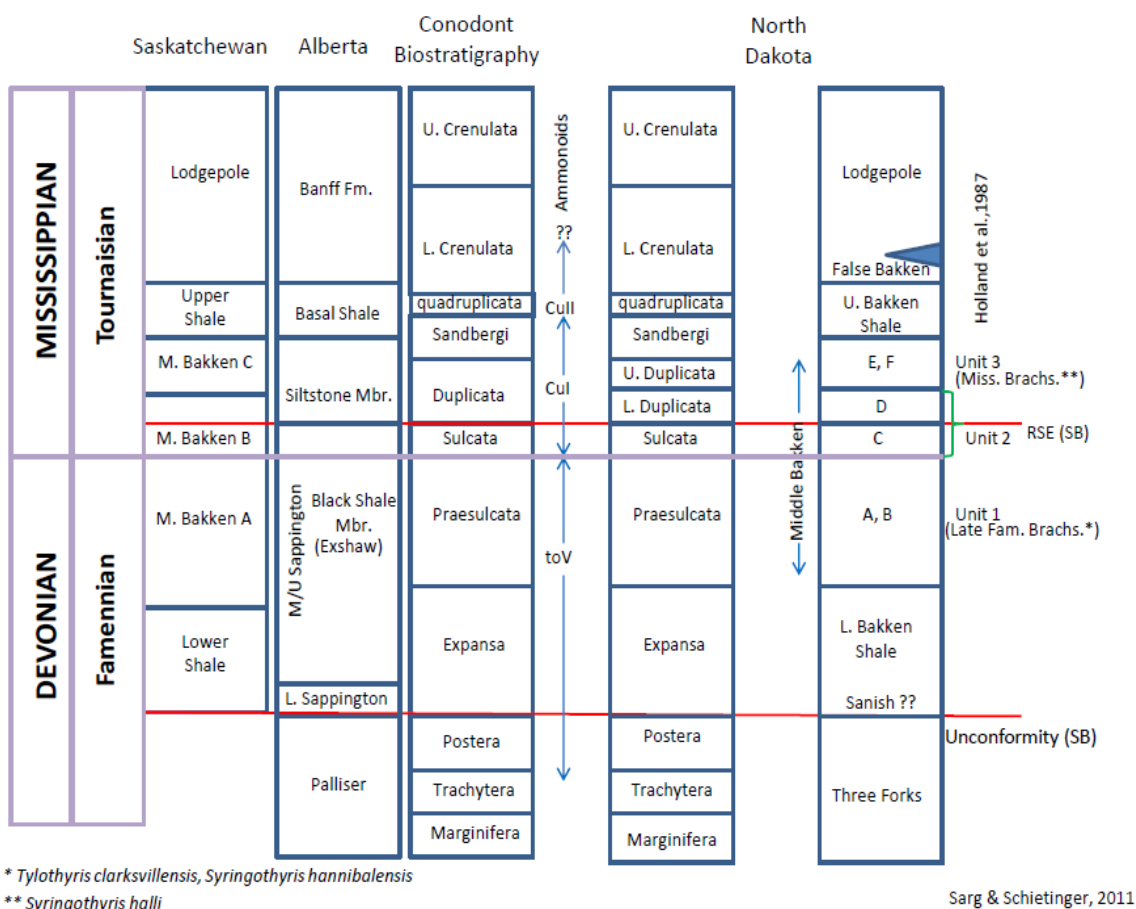


Figure 13. Biostratigraphic summary for the greater Williston basin area.

The Bakken Formation consists of three members: upper and lower organic-rich black shales and a middle member that varies in composition from a silty dolostone or limestone to a sandstone lithology (LeFever et al., 1991). The total Bakken thickness ranges from upwards of 140 feet (42.7 meters) thick in the center of the basin to a zero pinchout at the edges of the basin. The limits of the three Bakken members have been mapped showing the pinch out of each the Bakken members toward the basin margins (Webster, 1984). The lower member consists of dark gray to brownish black to black, massive to fissile, slightly to highly organic-rich shale (Pitman et al., 2001). The upper member is lithologically similar to the lower member and consists of dark gray to brownish black to black, fissile, slightly calcareous, organic-rich shale. The upper

member differs from the lower member in that it lacks crystallized limestone and greenish gray shale beds and has a higher organic matter content (Pitman et al., 2001). These upper and lower shales have been interpreted to have been deposited in an offshore marine environment during periods of sea-level rise (Pitman et al., 2001; Webster 1984). Webster (1984) and Lineback and Davidson (1982) provided evidence that both of these shales were deposited in a stratified hydrologic regime indicated by the lack of benthic fauna, presence of pyrite, and high organic matter.

The middle member is highly variable and consists of a light gray to medium-dark gray, interbedded sequence of siltstones and sandstones with lesser amounts of shale, dolostones, and limestones rich in silt, sand, and oolites (Pitman et al., 2001). This middle member has been interpreted to have been deposited in a shallow water marine depositional environment (Smith and Bustin, 1996). The Middle Bakken Member has been divided into lithofacies A-F as described above, and these facies provide the framework for a sequence stratigraphic interpretation of the Bakken stratigraphic system. Figure 14 illustrates a typical well with the different lithofacies and significant sequence bounding surfaces identified. The following figures 15 and 16 are two example cross-sections from different parts of the basin. Figure 15 is a regional cross-section in the central Williston basin near the Canada-USA border, and Figure 16 is an east-west cross-section across the Sanish to Parshall field areas.

The Bakken Formation comprises two depositional sequences that are, from the base upward, (1) a sequence that begins with the tectonically enhanced unconformity at the top of the Three Forks Formation (Figure 14) and is overlain by a transgressive system that is composed of the lower portion of the Lower Bakken Shale. The top of low density values mid-way through the shale is interpreted as a maximum flood surface, and is overlain by highstand systems tract that includes the upper portion of the Lower Bakken Shale and facies A, B, and C of the Middle Bakken Member. The shift to lower density is probably a shift to higher organic content within the shale, signaling higher preservation of organic matter as the basin deepens during transgression. The highstand systems tract is characterized by shallowing upwards from deeper water shale to skeletal wackestone, to burrowed siltstone and wackestone of an outer ramp environment to a laminated siltstone that shows some tidal influence and is interpreted here to represent a proximal outer ramp environment. The first Bakken sequence is ended by a mildly erosional and sharp sequence bounding surface that occurs at the base of the D facies. The D facies is characterized by cross-bedding and coarser texture, quartz sandstones or ooid grainstones, and is interpreted to be a high-energy, shoaling facies. The D facies is variable in thickness and aerial extent, and probably represents a series of down-ramp shoreline deposits (Figure 15 and 16). The D facies is interpreted to be the lowstand systems tract of the second Bakken sequence. The succeeding E and F facies comprise a return to deeper, subaqueous deposition and are a deepening upward transgressive systems tract. The maximum flooding surface again occurs within the Upper Bakken Shale at another shift to lower density and a high gamma ray value (Figure 14). The overlying highstand of this sequence includes the upper part of the Upper Shale and the lower portion of the Lodgepole Formation.

Lear Pet Expl Parshall SD 1  
Sec. 3-T152N-R90W

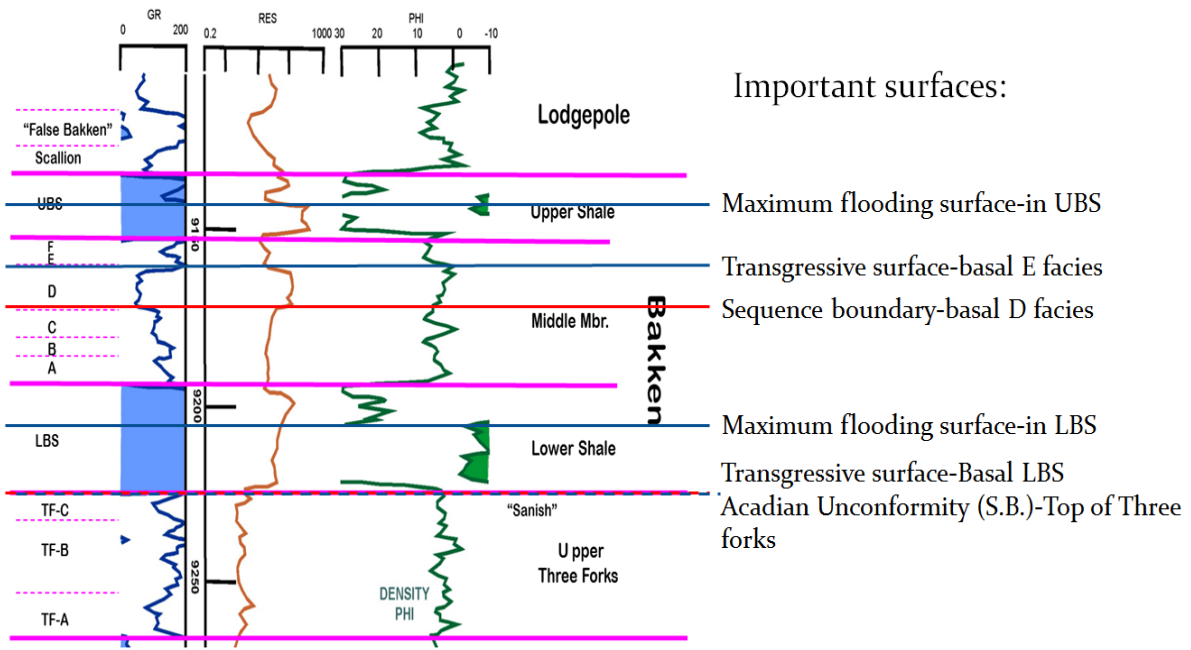


Figure 14. Wireline log for the Well Parshall SD-1 with sequence stratigraphic interpretation of important surfaces for the Bakken Formation (modified from Sonnenberg et al, 2011).

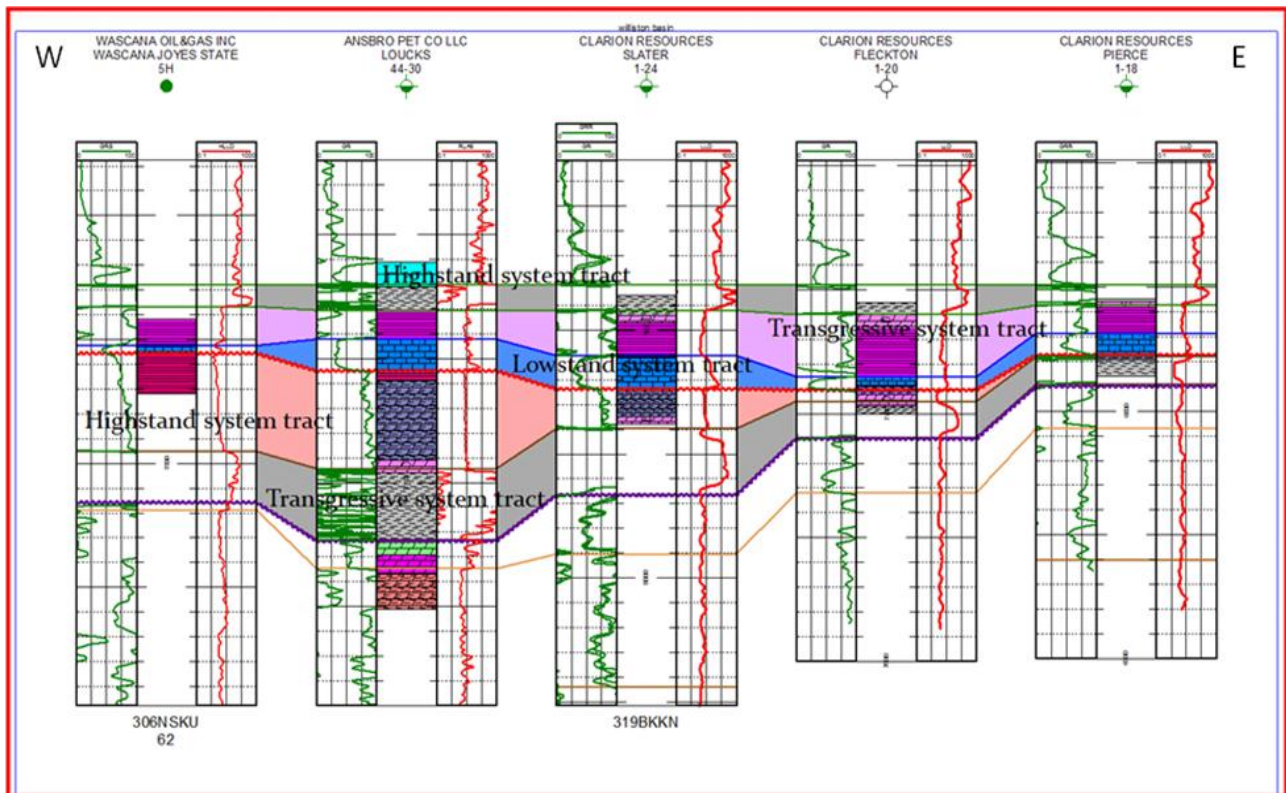


Figure 15. Cross-section across the Williston Basin with systems tracts and sequence boundaries illustrated (modified from Sonnenberg et al., 2011).

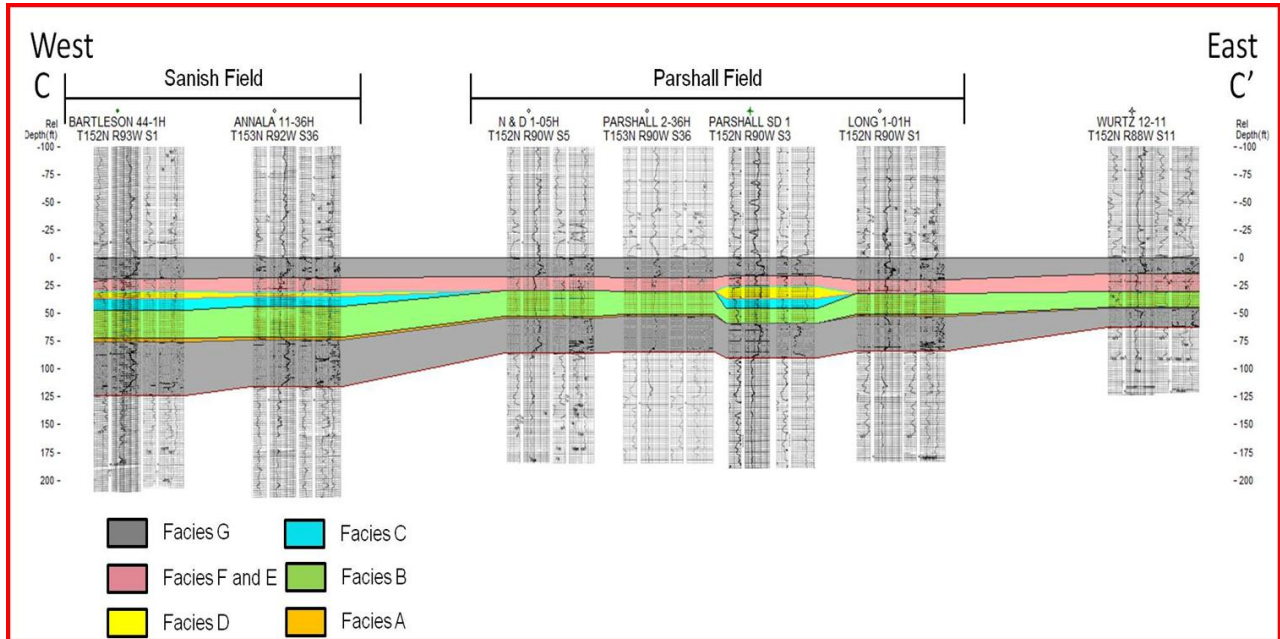


Figure 16. West to east stratigraphic cross-section with top Upper Bakken Shale as datum (from Simonsen, 2010). Lower Bakken Shale and Middle Bakken facies A, B, and C thin to the east toward the basin margin. Facies D is discontinuous and its basal contact is in erosional contact with underlying facies C.

### Mineralogy and Reservoir Quality:

Quantitative mineralogy for the Bakken Formation was done in the CSM Advanced Mineralogy Research Center using QEMSCAN. This is a scanning electron microscope (SEM) system that was initially designed for the metals mining industry, to optimize metallurgical and mining operations (Hoal et al., 2009a). It provides rapid, automated quantitative mineral analysis and data acquisition for thousands of grains in a short time (Hoal et al., 2007). It is a nondestructive analysis process that ensures objectivity and repeatability (FEI, 2010). It is used to understand mineralogy, texture, and mineral associations (Hoal et al., 2009a).

The system combines a fully automated Carl Zeiss EVO50 scanning electron microscope with four Bruker silicon-drift energy dispersive (EDS) x-ray detectors, an energy resolution of 133 eV (Mn K), a four quadrant solid-state backscatter electron detector, a secondary electron detector, and 1000-count combined x-ray counts per determination (Hoal et al., 2009a). The array of four EDS-detectors allows for fast acquisition of data (commonly 150 analyses per second) and allows for the automated analysis of large samples for delivering statistically reliable data sets (Hoal et al., 2009b). The electron beam is automated through the iMeasure software at a user-defined pixel resolution (Hoal et al., 2009b). This study uses a 2 micrometer ( $\mu\text{m}$ ) resolution for porosity measurements, 30  $\mu\text{m}$  resolution for mineral percentage measurements, and 5  $\mu\text{m}$  for mineralogy textures.

During analysis, the system collects a backscattered electron (BSE) signal and EDS spectrum at each pixel location. The system then correlates them with x-ray and BSE count-based mineral definitions developed for the project (Hoal et al., 2009a). The final product is a false-colored image of the sample with a large data set that can be queried and displayed according to project objectives (Hoal et al., 2009a).

The mineralogy across all the Middle Bakken lithofacies is very similar and is dominated by dolomite, calcite, and quartz (Kowalski, 2010). The Bakken 'shales' show a diverse mineralogy and are quartz-rich (40-90% by volume). This, plus the carbonate content (5-40%), may play a significant role in making the Bakken shale brittle and thus able to open and maintain natural micro-fractures as well as induced hydro-fractures from well completion. The following Figures 17-24 summarize typical mineralogy for the Bakken shales and the Middle Bakken Member facies.

- Bakken shales (Figure 17) range from 5 to 85% quartz and is comprised of both quartz silt and siliceous microfossils. The quartz shows a consistent increase from the base of each shale, to the middle of each unit, and then a progressive decrease in quartz in the upper part of the shale. Clay content shows a compensatory decrease and then increase throughout each of the shale units.
- Facies A (Figure 18) is composed predominantly of quartz (35-40%) and calcite (42-47%) with minor amounts of clay and other minerals.
- Facies B (Figures 19 and 20) is rich in quartz (30-50%) and calcite (10-50%), with lesser dolomite (5-20%), and clay plus feldspar (15-25%). Dolomite can range to higher amounts such as at Elm Coulee where it can be greater than 50% of the rock (Alexandre, 2011).
- Facies C (Figures 19 and 21) is composed of quartz (20-45%) and calcite (2-50%), dolomite (12-35%), and clay plus feldspar (7-25%).
- Facies D (Figures 19 and 22) is rich in calcite (30-75%) which is present as both grains and cement and quartz (15-45%), with lesser amounts of dolomite (3-10%) and clay plus feldspar (3-10%). Facies D generally appears to be well cemented early in its history and is only mildly dolomitized.
- Facies E (Figures 19 and 23) is dominantly quartz (25-40%) and dolomite (27-42%) with smaller amounts of clay (10-25%) and calcite (1-25%). The significant amount of dolomite makes this facies an attractive hydro-fracturing target in the Sanish-Parshall fields.
- Facies F (Figure 24) is also rich in quartz (20-45%) and dolomite (30-50%), and has lesser amounts of clay plus feldspar (7-25%) and calcite (2-37%).

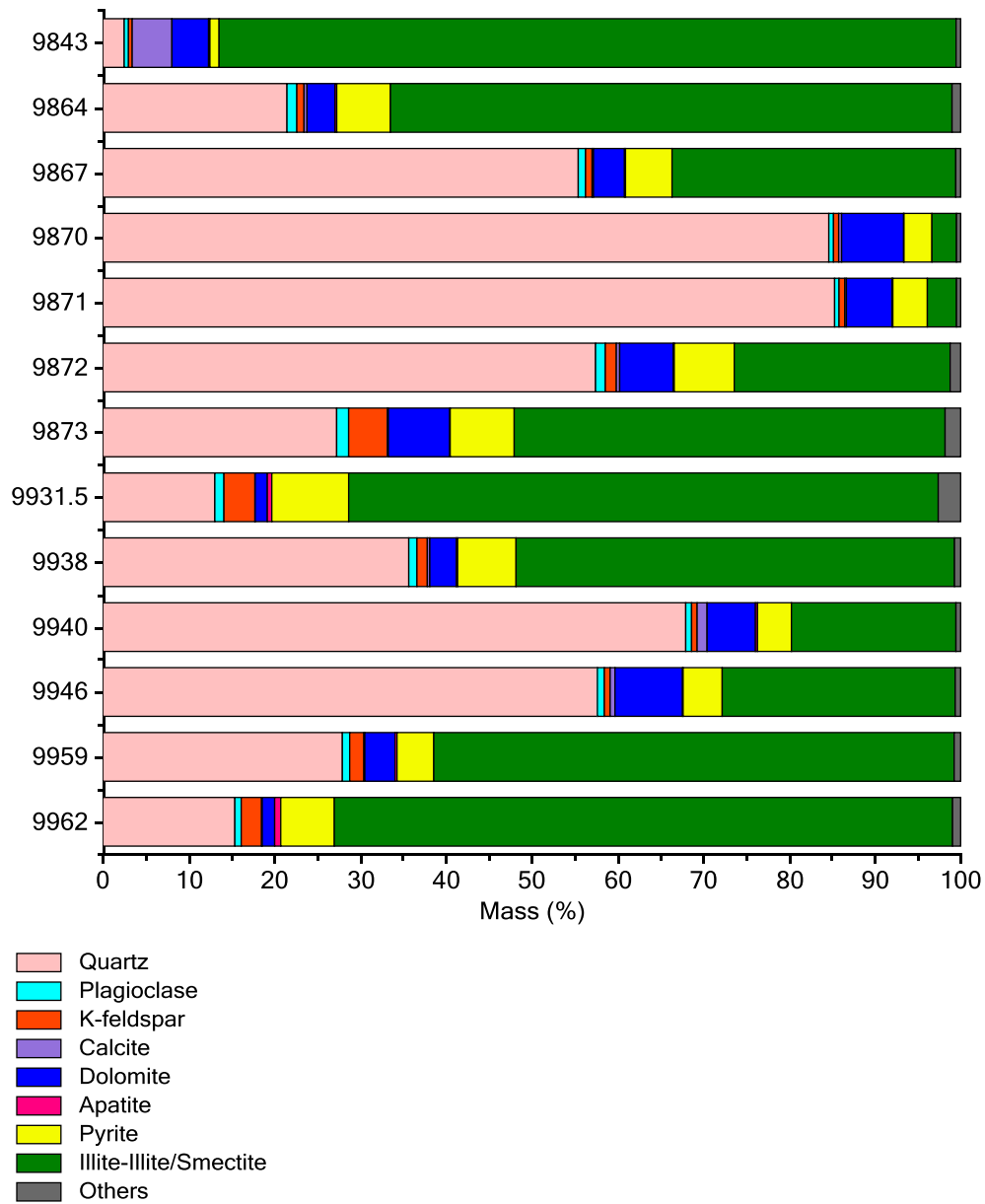


Figure 17. QEMSCAN analyses for Upper (9843-9873) and Lower (9931.5-9962) Bakken Shale.

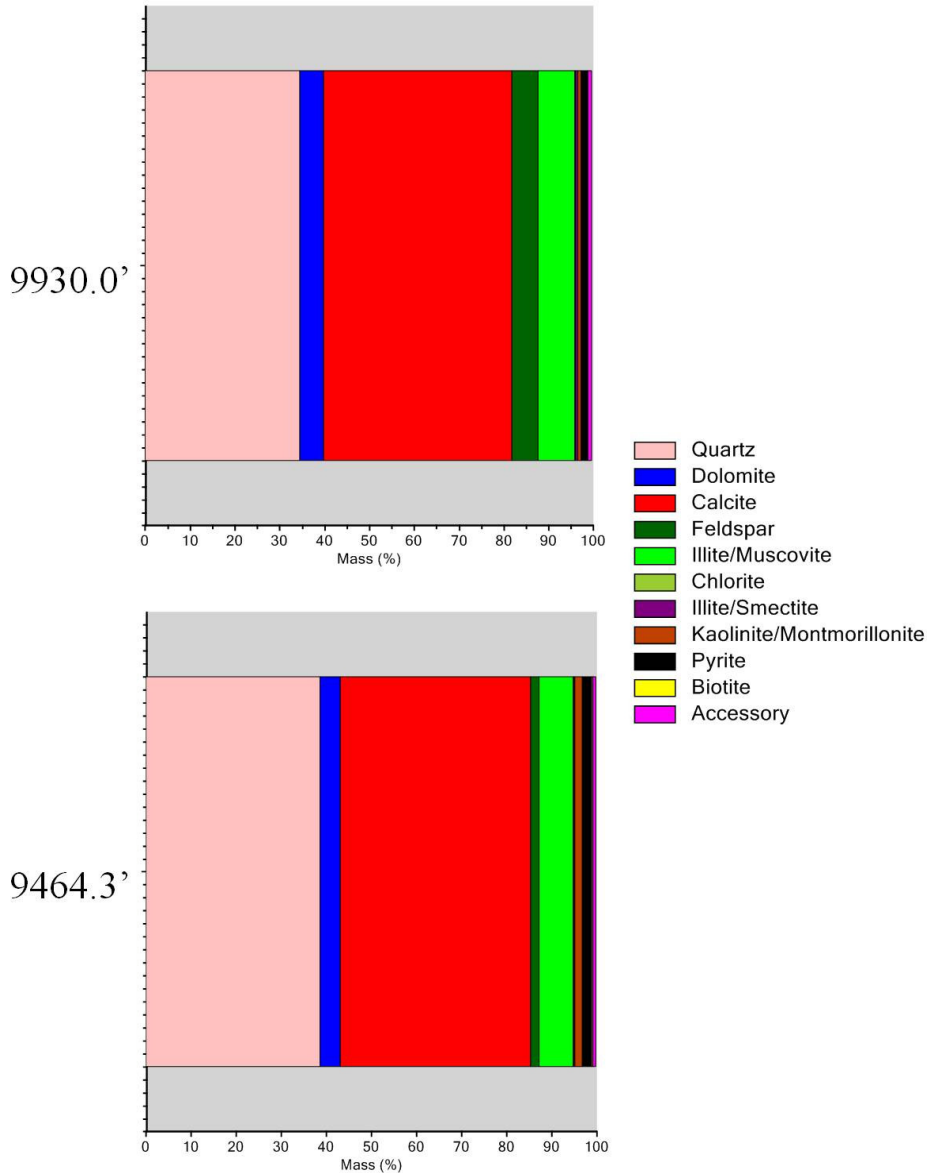


Figure 18. Bar charts showing mineral percentages for facies A. Top chart is from Braaflat 11-11 and the bottom chart is from N&D 1-05.

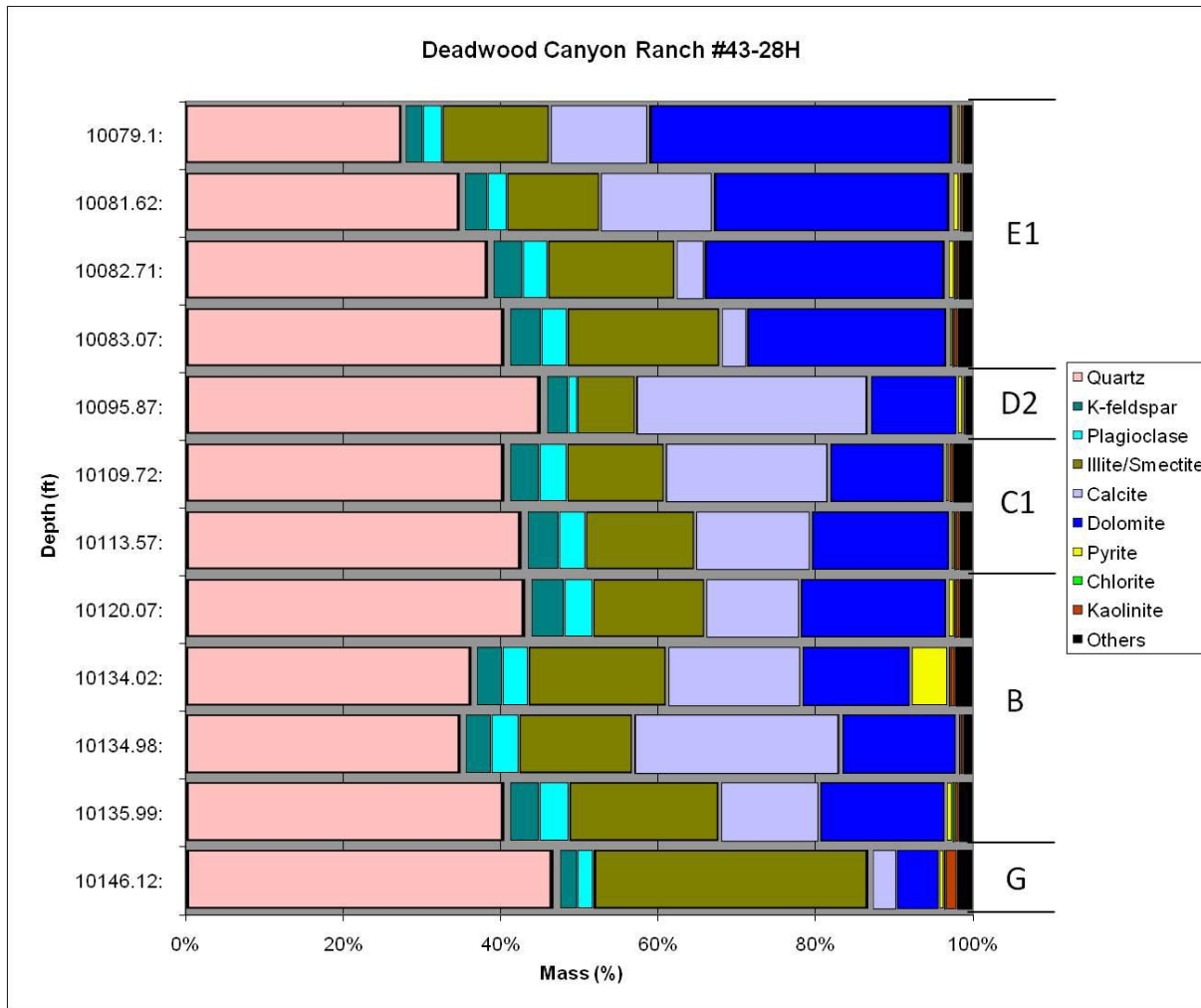


Figure 19. Mineralogical analysis measured from QEMSCAN for the Deadwood Canyon Ranch #43-28H core samples, Mountrail County, North Dakota.

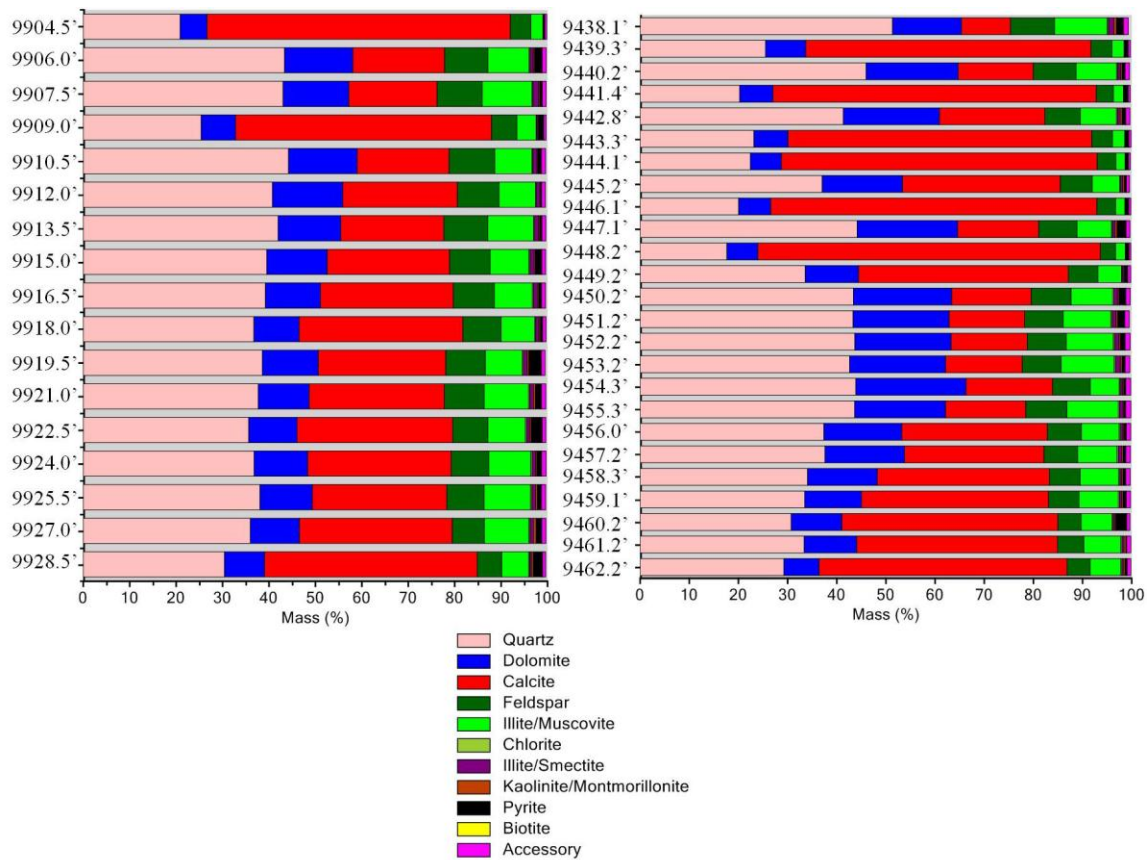


Figure 20. Bar charts showing mineralogy for facies B. Data on the left are from Braaflat 11-11 and the right-hand data are from N&D 1-05.

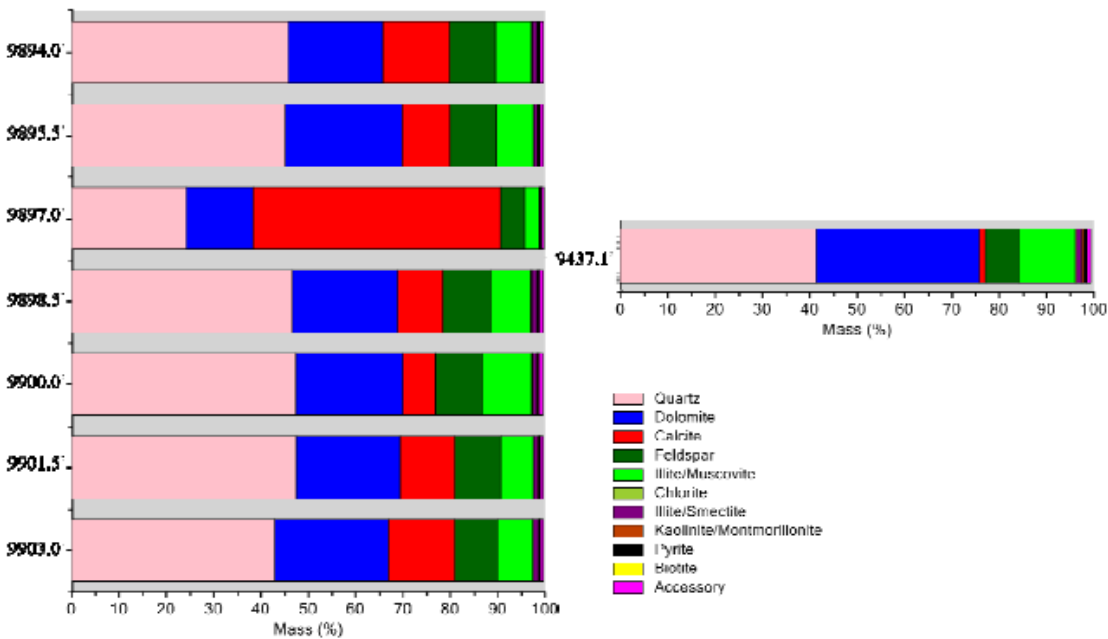


Figure 21. Bar charts showing the mineralogy for facies C. Left-hand data are from Braaflat 11-11 and the right-hand data are from N&D 1-05

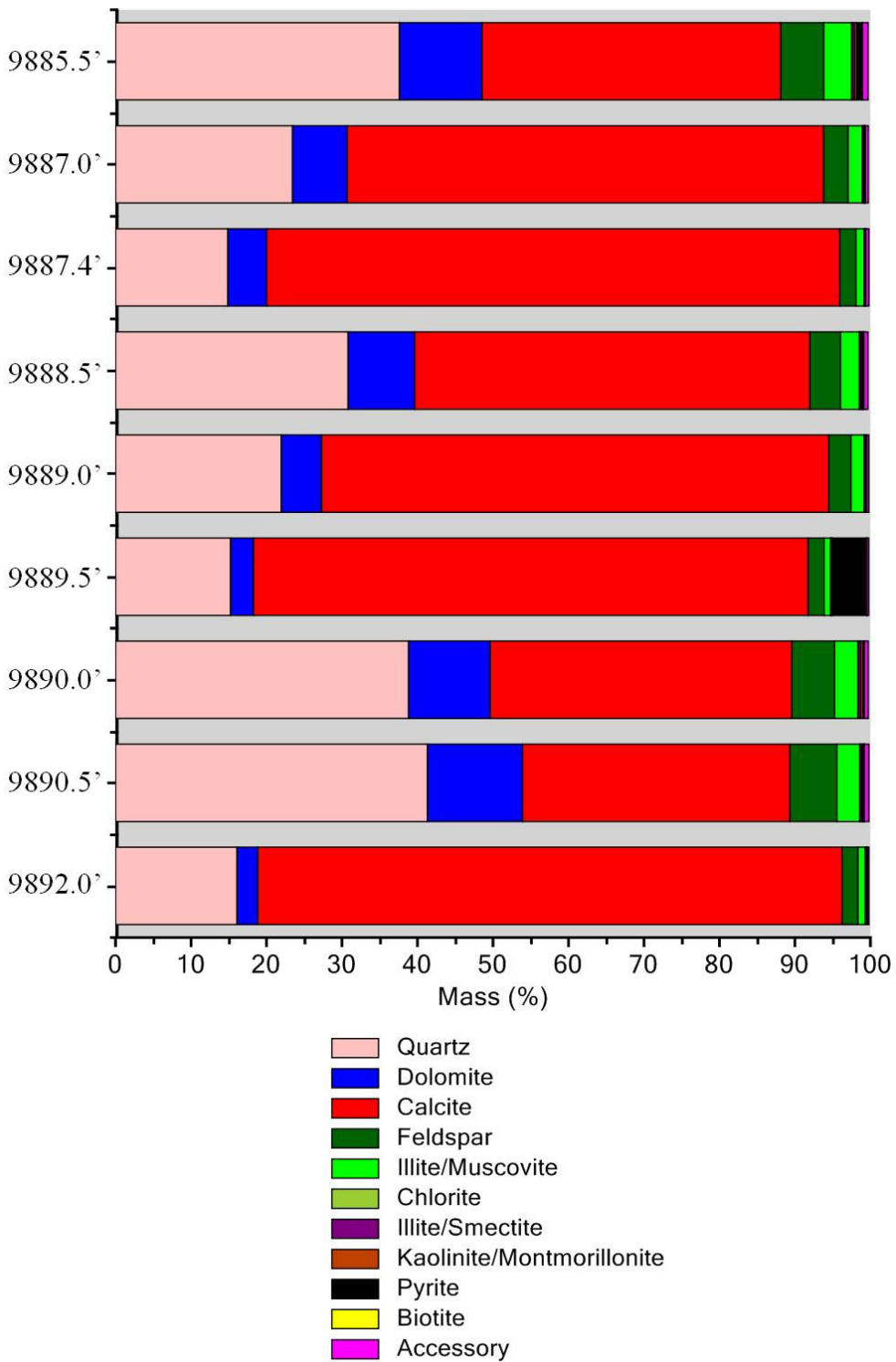


Figure 22. Bar charts showing the mineralogy for facies D in Braaflat 11-11. Notice the 3 cycles of decreasing calcite and increasing quartz and dolomite. Facies D is absent in N&D 1-05.

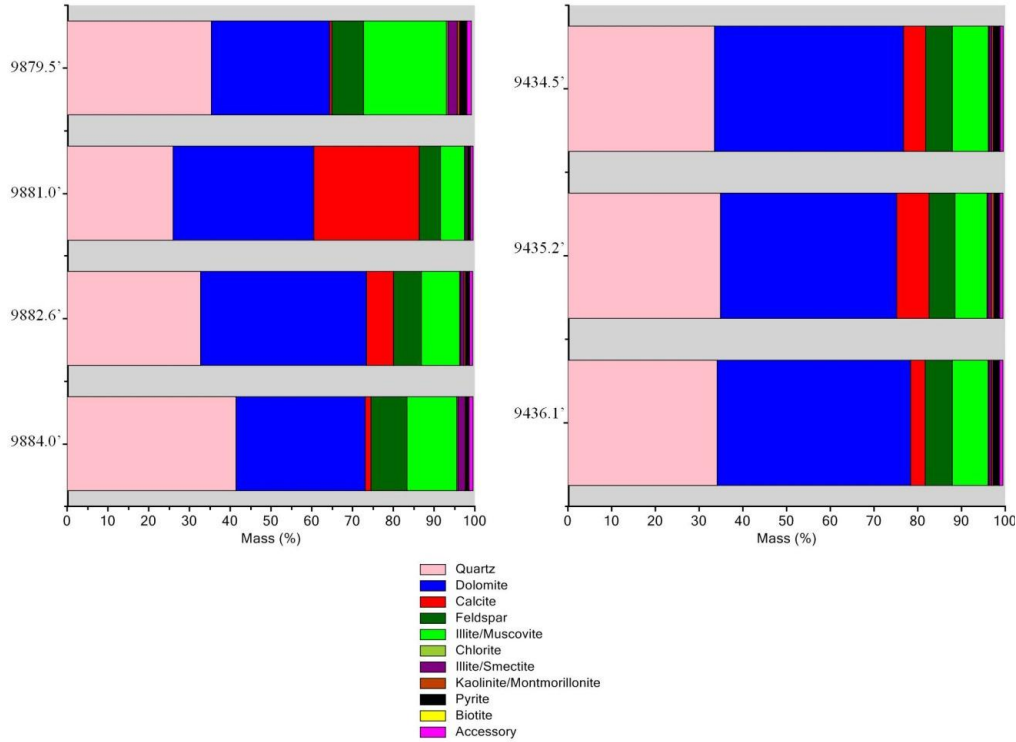


Figure 23. Bar charts showing the mineralogy of facies E. Data on the left are Braaflat 11-11 and the data on the right are from N&D 1-05.

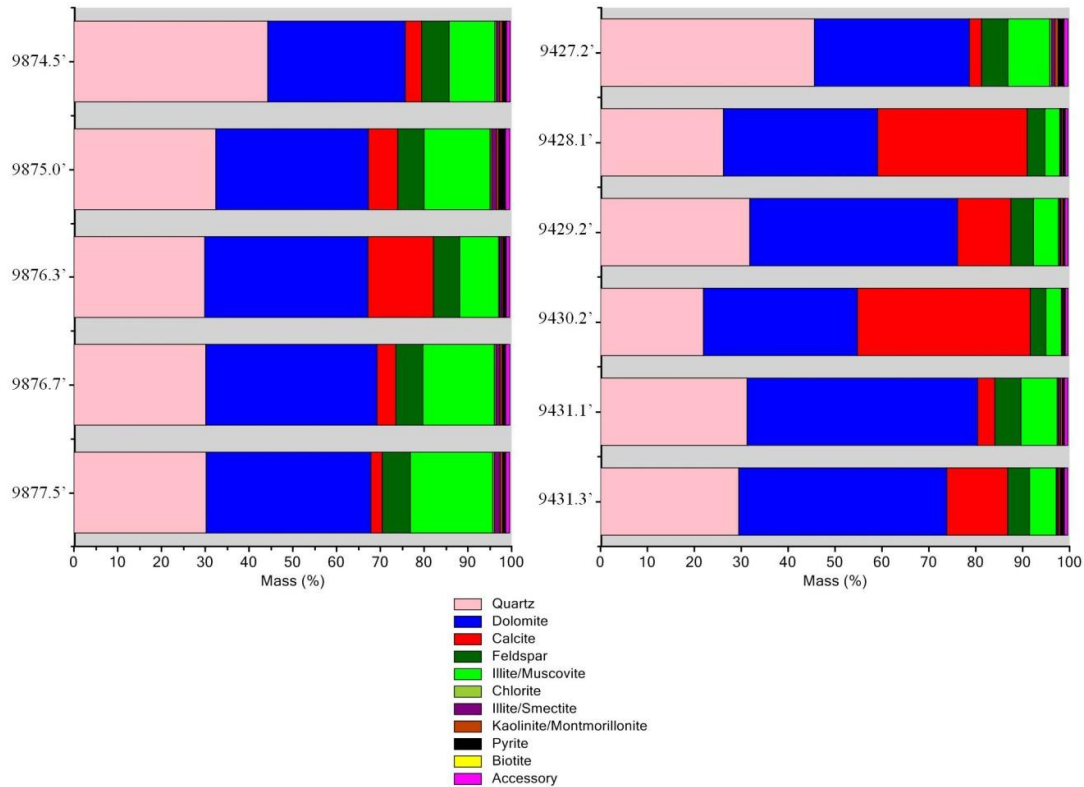


Figure 24. Bar charts showing the mineralogy of facies F. Data on the left are from Braaflat 11-11 and the data on the right are from N&D 1-05.

In summary:

1. The Bakken Formation is comprised of a shallow to deep marine ramp system that is composed of two depositional sequences that are correlated across the Williston basin.
2. Middle Bakken facies B, C, D, and E can all be reservoirs, if quartz and dolomite-rich (facies D) or dolomitized (facies B, C, E).
3. Porosity averages 4-8%, permeability averages 0.001-0.01 mD or less.
4. Matrix reservoir quality is enhanced by dolomitization. Porosity is intercrystalline and tends to be greater than 6%. Permeability may reach to 0.15 md or greater. This is a “sweet spot” determinant (e.g., Elm Coulee, Parshall, and Sanish).
5. The Upper Bakken Shale is siliceous, which increases brittleness and enhances hydro-fracturing potential.

## **ROCK PHYSICS, ANISOTROPY, AND ORGANIC MATURITY**

Published data on all organic-rich shale, including the Bakken shale was analyzed to understand the different controls on seismic velocities. The correlation between kerogen content and elastic properties is significantly better if porosity-modified kerogen content is used. An inverse empirical correlation exists between stiffness and porosity-modified kerogen content. The upper and lower Bakken are strongly anisotropic. The anisotropic properties of the shales were analyzed, and there are differences between the Young’s modulus measured parallel and perpendicular to bedding. The variation between vertical and horizontal Young’s modulus results in a strikingly different horizontal stress profile. The apparent increased horizontal stress in the Upper and Lower Bakken shale imply that they will be much more effective in hydro-fracture containment. Any vertical fractures will tend to close. However, horizontal bedding plane partings and horizontal micro-fractures generated due to hydrocarbon maturation and expulsion are common in the Bakken shales and may allow fracture expansion during hydro-fracturing. To test this hypothesis, elastic property measurements were conducted on a series of core samples from the Freda Lake Field, in southern Saskatchewan (Havens, 2012).

The effective minimum horizontal stress is a primary controller of fracture growth. Knowledge of the elastic properties and Biot’s poroelastic coefficients is required to accurately determine the effective minimum horizontal stress. In this study, dry rock velocities were measured for four geologic facies from the Middle Bakken Member and one from the Lodgepole Formation. Mineralogy data was also obtained for the rocks measured in the laboratory. This data along with available literature measurements in the Bakken shale allows for estimation of in-situ dry rock elastic constants and Biot’s coefficients.

The dry rock stiffness tensor was determined by treating the dipole shear log as a dry rock measurement. Empirical equations were then derived from laboratory data and applied to the shear waves to predict the remaining components of the stiffness tensor. Fluid substitution was performed with Gassmann’s equation to acquire the saturated stiffness tensor.

Biot’s coefficients were calculated using the dry rock stiffness tensor and an estimate of the mineral bulk modulus by assuming a Voigt-Reuss-Hill effective medium for the pure grain moduli.

Biot's coefficients describe the ability of the pore pressure to counteract the outward stresses on the rock and will be between zero and one. The values for all formations in this study were well below one and ranged from 0.15-0.75 over the unit of interest.

The saturated stiffness tensor and Biot's coefficients were input into the effective minimum horizontal stress equation assuming uniaxial strain. The stress profile showed no major contrast over the area of interest (Figure 25). A slight decrease in horizontal stress was observed in the common reservoir facies of the Middle Bakken, but the remaining units all had similar horizontal stress.

Mini-Frac tests were performed in the Upper Bakken Shale and the Scallion Member of the Lodgepole Formation. The tests provide estimates of reservoir pressure, total minimum horizontal stress, tensile strength, and total maximum horizontal stress. The interpreted stress from the Mini-Frac tests matched well with the modeled results, and showed low stress contrast between the Upper Bakken Shale and Scallion Member (Figure 25).

A total minimum horizontal stress profile was provided by Schlumberger for the same Freda Lake well along with transversely isotropic elastic properties (Figure 25). The stress profile was only able to predict the Mini-Frac test in the Upper Bakken Shale, and a calculation of Thomsen anisotropy parameters (Thomsen, 1986) showed the  $\delta$  parameter in the Bakken Shales ranged from 0.5-1.2. These  $\delta$  values are much higher than any existing anisotropy measurements in the Bakken Shales (Vernik & Nur, 1992). The likely cause for the high values is an attempt by Schlumberger to match the Mini-Frac tests by adjusting the anisotropy and disregarding the possibility of Biot's coefficients less than unity. This leads to a massive stress contrast in the Bakken shales that would ultimately be interpreted as a strong fracture barrier.

The in-situ pressure testing and modeled results show low stress contrast throughout the unit of interest. The analysis by Schlumberger predicted a contrasting stress profile, but the input parameters were unrealistic and the profile did not match in-situ pressure testing. This demonstrates the importance of estimating accurate Biot's coefficients and realistic anisotropy parameters. Instead of acting as containment for fracturing, the Bakken Shale may, in fact, fracture in response to hydro-fracturing during well completion. These induced fractures will enhance permeability between micro-fractures in the Bakken Shale, which are generated by hydrocarbon maturation and expulsion and may contribute hydrocarbons to well production when the immediately underlying Middle Bakken is hydro-fractured during well completion.

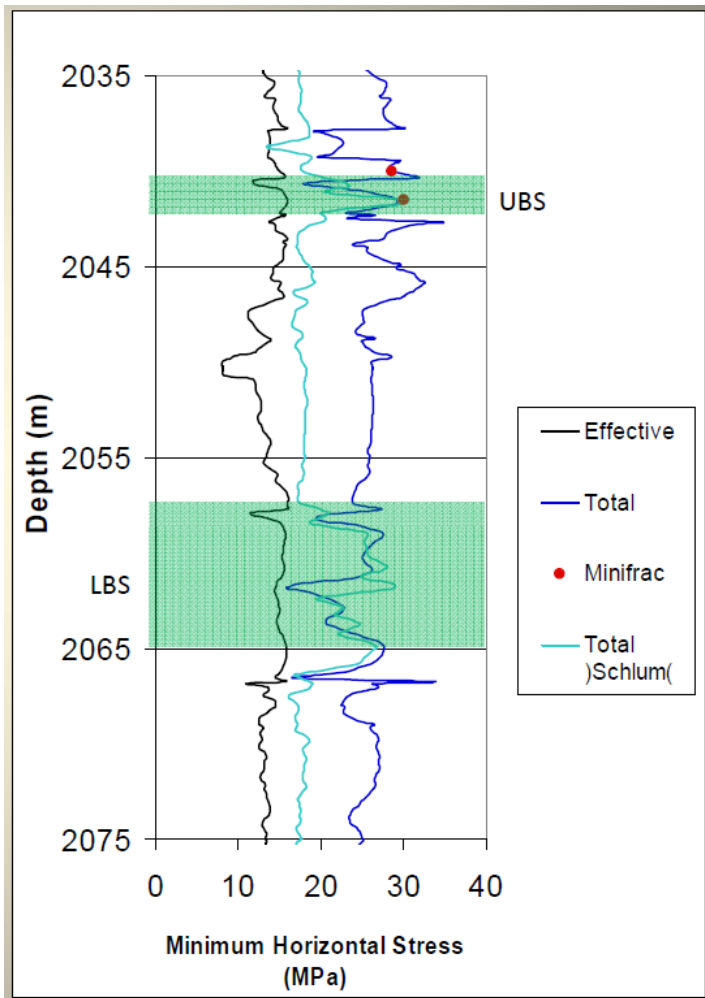


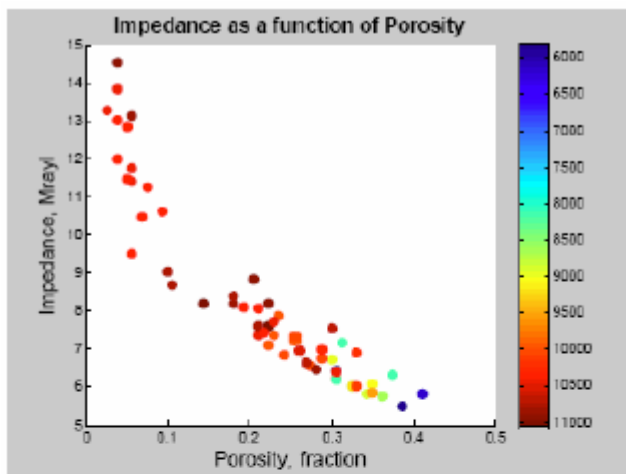
Figure 25. The calculated effective and total minimum horizontal stress is shown in black and blue. The total minimum horizontal stress determined by Schlumberger is shown in light green, and the Mini-Frac test results are the red dots. Upper Bakken (UBS) and Lower Bakken (LBS) Shale are green layers. Middle Bakken Member occurs between UBS and LBS.

The relationship between organic maturation and seismic impedance were investigated. Organic matter, pore space (i.e., lamina parallel microfractures in Bakken shale), and clay content are all contributors to organic-rich shale (ORS) impedance values. Nano-indentation was performed on eleven (11) Bakken Shale samples – 6 from the Upper Shale and 5 from the Lower Shale. Based on literature values, a threshold of 33GPa was set as the upper boundary for average Young's Modulus for the soft shale components (clay and kerogen). The sample maturities were determined by pyrolysis, and cross plots were made of total organic carbon (TOC), Hydrogen Index (HI), transformation ratio (TR) and the maximum temperature at S2 pyrolysis (TMax). Correlation coefficients for the linear trends were 0.77, 0.72, 0.82 and 0.70 respectively. These data were combined with analysis of 47 wells from across the basin to define relationships between maturity-dependent rock properties.

These data show a number of trends:

- There is a non-linear, reduction in impedance with increasing porosity, but the relationship becomes linear when porosity is added to TOC (Figure 26).
- Young's Modulus (measure of stiffness) increases with maturity for the soft components (Figures 27, 28, and 29).
  - Young's Modulus increases with increasing HI, a measure of maturity (Figure 27).
  - There is an increase in median Young's Modulus of kerogen plus clay with increasing TR, and there is a linear positive correlation between impedance and the transformational ratio (TR, measure of generated hydrocarbons) (Figure 28).
  - Similarly, as Tmax increases, both Young's Modulus of kerogen plus clay and impedance increase (Figure 29).

Thus, an increase in Young's Modulus with maturity correlates to an increase in impedance. Although a reduction in porosity is expected with increasing depth and maturity, if the maturation process results in lamina parallel micro-fracturing, this will dampen but not eliminate the general trend to lower porosity with burial. Since trends in clay and kerogen stiffness, and porosity are similar, maturity level is directly related to impedance of ORS shales.



A.

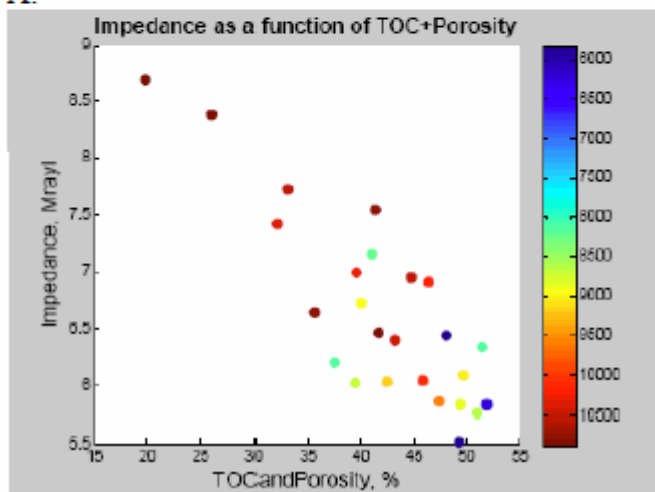


Figure 26. A. Non-linear reduction in impedance with increasing porosity. B. Linear reduction in impedance with increasing porosity plus TOC.

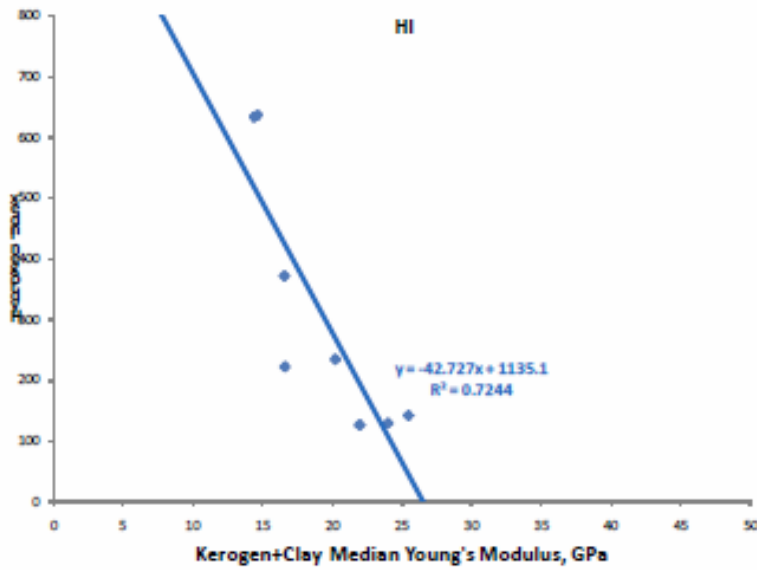


Figure 27. Plot of HI versus organic- rich shale soft components (kerogen and clay). Young's Modulus increases with maturity.

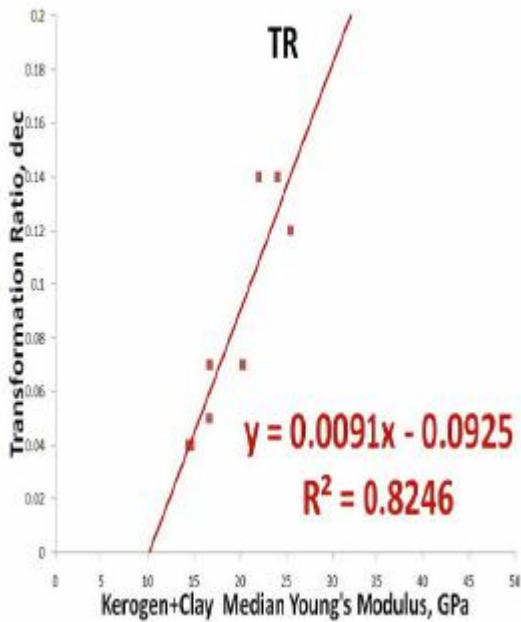


Figure 28. Plot of TR versus organic-rich shale soft components. Young's Modulus increases with TR and maturity.

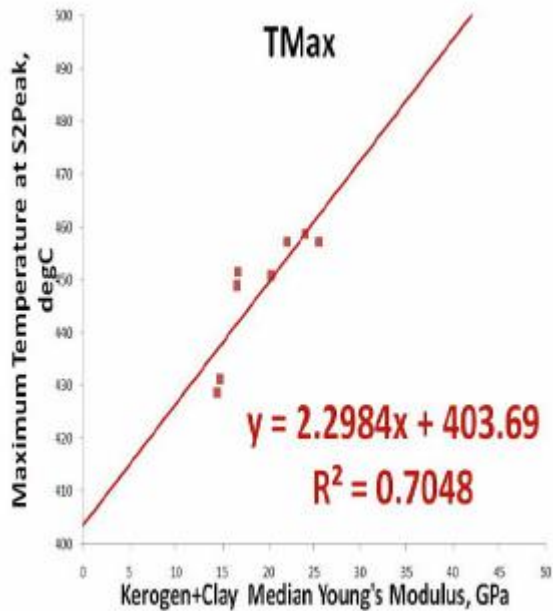


Figure 29. Plot of TMax versus organic-rich soft components. Young's Modulus increases with TMax and maturity.

In summary:

1. The Bakken shales and the Middle Bakken Member have similar effective stress suggesting that the shale will not contain induced fractures, and will contribute hydrocarbons from interconnected micro-fractures.
2. Organic-rich shale impedance will increase with a reduction in porosity, and an increase in kerogen stiffness during the burial maturation process, and thus, maturation can be directly related to impedance.

### SUB-REGIONAL FRACTURE ANALYSIS

Fractures enhance the reservoir quality of the tight Bakken reservoir and source rocks. Three types of **open fractures** occur in the Bakken: (1) structural-related tectonic fractures; (2) stress-related regional fractures; and (3) expulsion fractures associated with overpressure due to hydrocarbon generation (Sonnenberg et al., 2011). The best production comes from hydrocarbon generated related pervasive micro-fracturing within the Bakken combined with larger scale fracturing (i.e., structural-related or stress-related regional fractures).

Outcrop and core description documents smaller-scale field fracture systems, tied to the regional system. These data provide key documentation of potential reservoir heterogeneity. Fracture orientations, fracture density, and fracture lengths were mapped within Devonian/Mississippian strata of the Big Snowy and Little Rocky Mountains, Montana, and the Beartooth Range in Wyoming and Montana (Angster, 2010) (Figure 30). Preliminary results of field data show a relationship between bedding structure and fracture orientation (Figures 31-33) where local structure is the dominant control on fracture orientation. Analysis of a 3D seismic grid on the north end of

the Billings Nose in the Bicentennial field area (Figure 30) provides subsurface data that is integrated with the outcrop study and the literature (Figures 34-38) and is consistent with local fracture controls. Where local structure is absent or very gentle, a regional orthogonal NE-SW and NW-SE system of fractures is prevalent (Figures 32 and 35). These are enhanced when local structure is superimposed on the regional trends (Figures 34, 37-38).

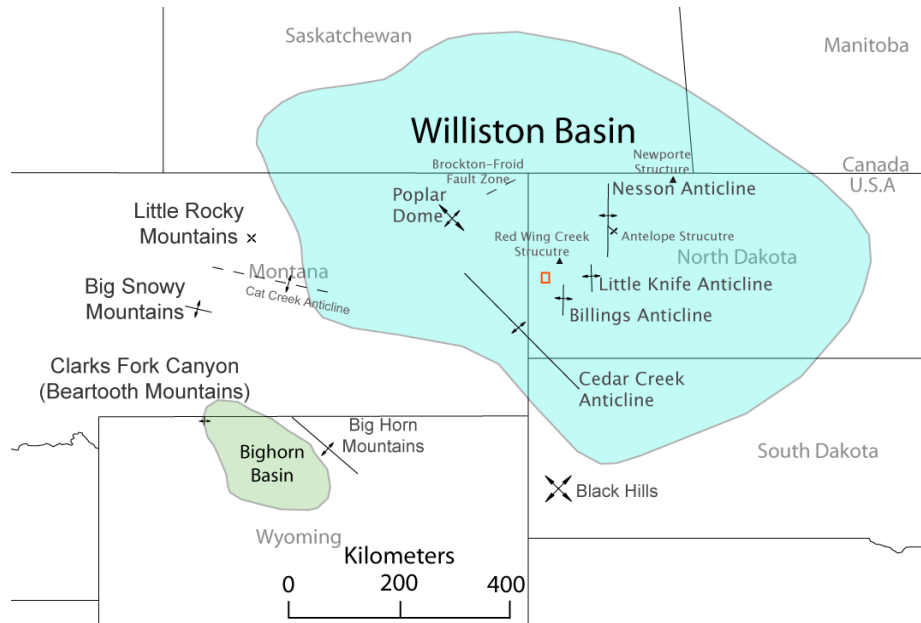
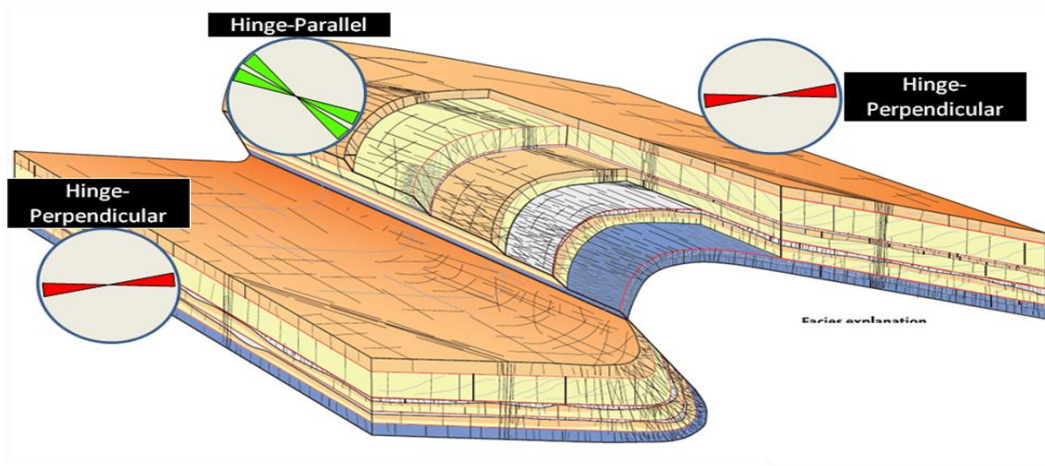


Figure 30. Base map showing location of seismic data (red box), and outcrop localities in Montana and northwestern Wyoming.



Modified from C. Zahm, P. Hennings, 2009

Figure 31. Structural model showing hinge or axis perpendicular or oblique and axis parallel fracture orientations.

**Structural-related tectonic fractures:** Several large fault-bounded anticlinal features, the Nesson and Cedar Creek anticlines, have had recurrent movement through geologic time. These large structural features are thought to exert controls on the orientation of fractures in various reservoirs (Figure 31). The fractured reservoir in the Antelope field is thought to be the result of

sharp folding of the Antelope structure (Murray, 1968). Three-dimensional strain modeling of the Big Snowy Mountains show maximum strain at the two plunging ends of the anticline, and along the maximum curvature of the structure. This is consistent with the trend of high production wells along the sharp limb of the Antelope field anticline.

Structurally produced fracture sets are evident in both hinge perpendicular or oblique and hinge parallel orientations within the Big Snowy and Clarks Fork Canyon outcrops (Figure 32). These structurally induced fractures could be expected to overprint regional trends in structural areas within the Williston basin. This is evident in the Billings Nose, where this project has used curvature attribute analysis of 3D seismic data that shows axis perpendicular/oblique fractures overprinting the NE trending regional fractures (Figure 32, 34).

Mechanical stratigraphy analysis of the Bakken-equivalent, Cottonwood Canyon Formation at Clarks Fork Canyon of the Beartooth Mountains shows that hinge parallel and hinge perpendicular or oblique fractures are abundant in sandstone lithologies, and are rare in shale (Figure 33). Where present within the shale, the fractures are dominantly hinge perpendicular or oblique.

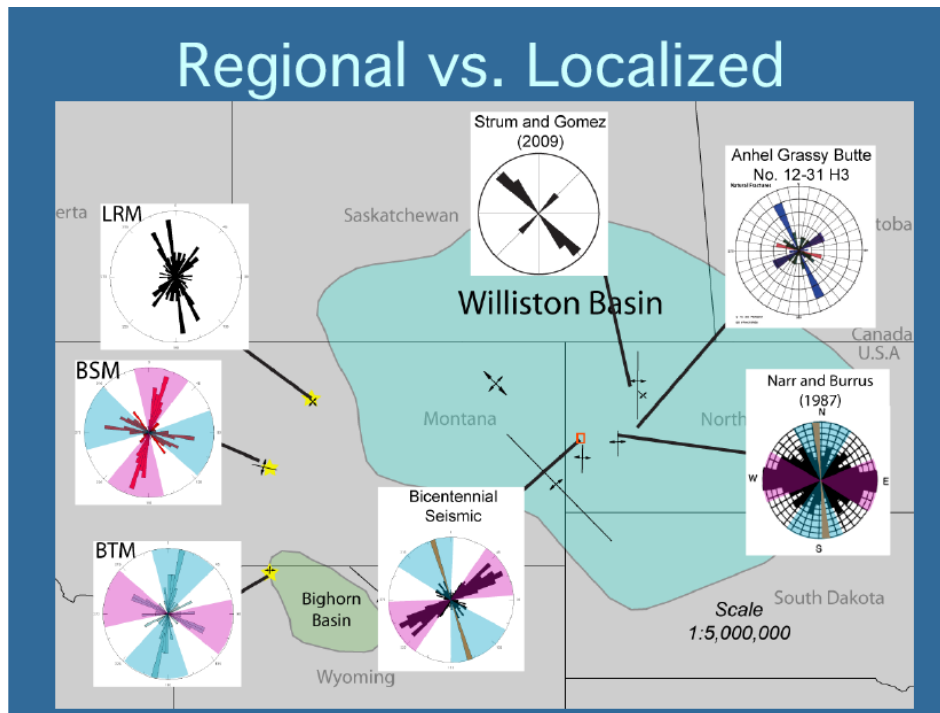


Figure 32. Synthesis of regional and localized fracture trends in Williston basin and surrounding environs (LRM-Little Rocky Mountains., BSM-Big Snowy Mountains., and BTM-Beartooth Mountains). Hinge perpendicular or oblique fracture trends are highlighted in lavender on the rose diagrams, and hinge parallel fracture trends are highlighted in blue. Regional trends are in the NE and NW directions (LRM, Strum & Gomez, and Anhel Grassy Butte), and will be enhanced where coincident with the local structure patterns.

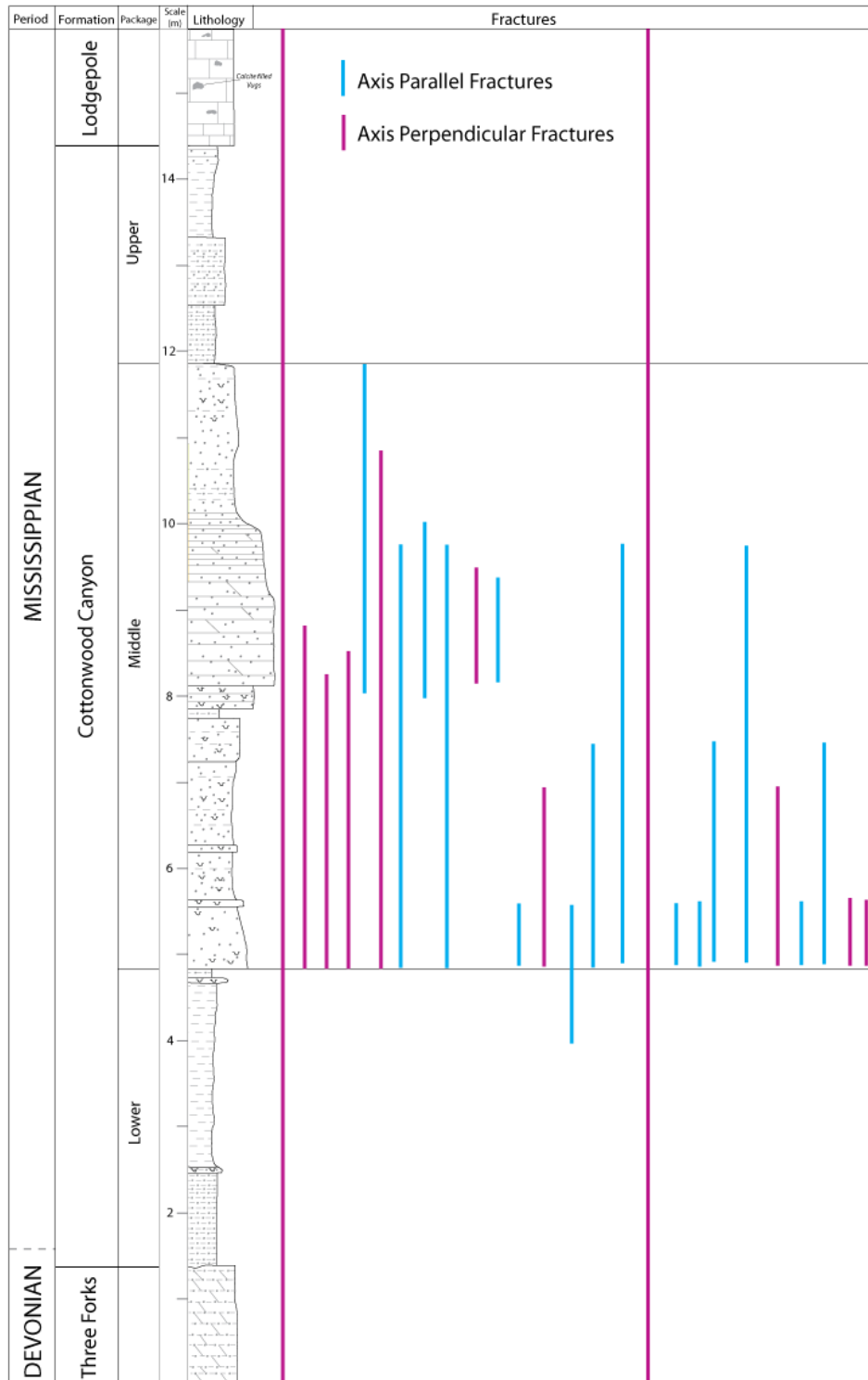
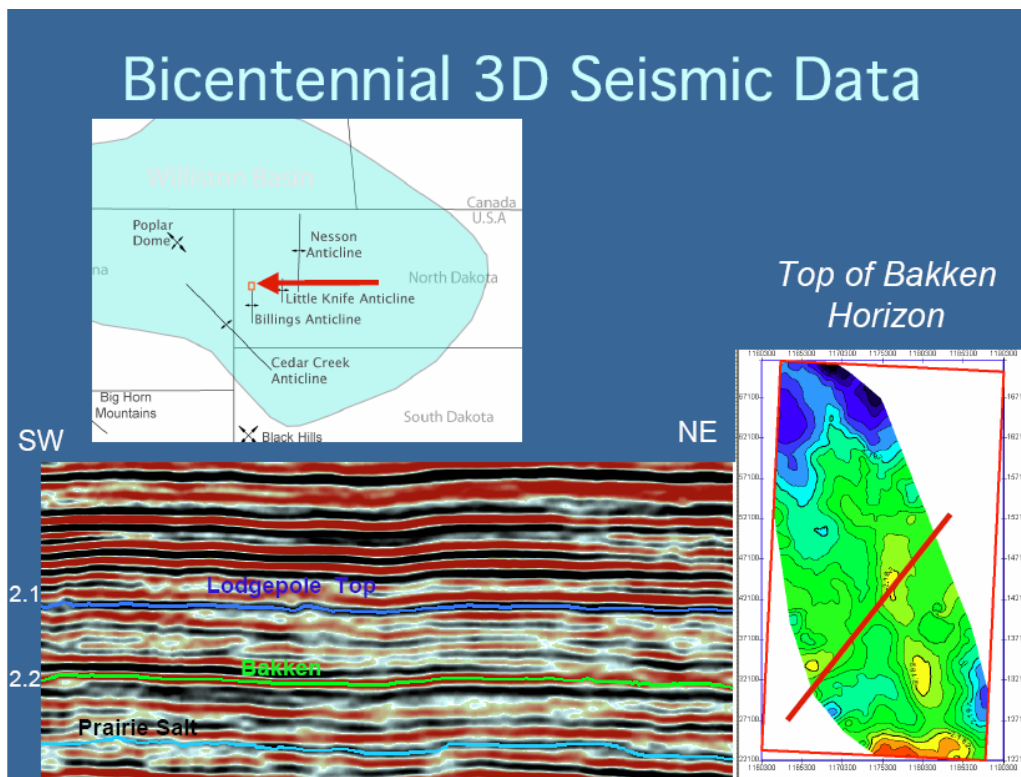


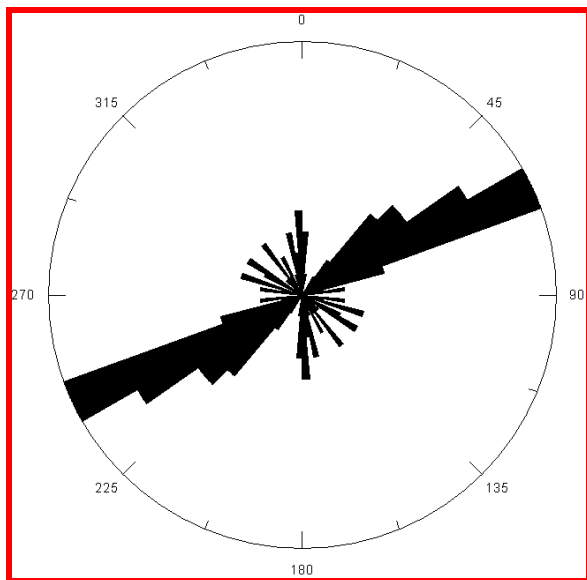
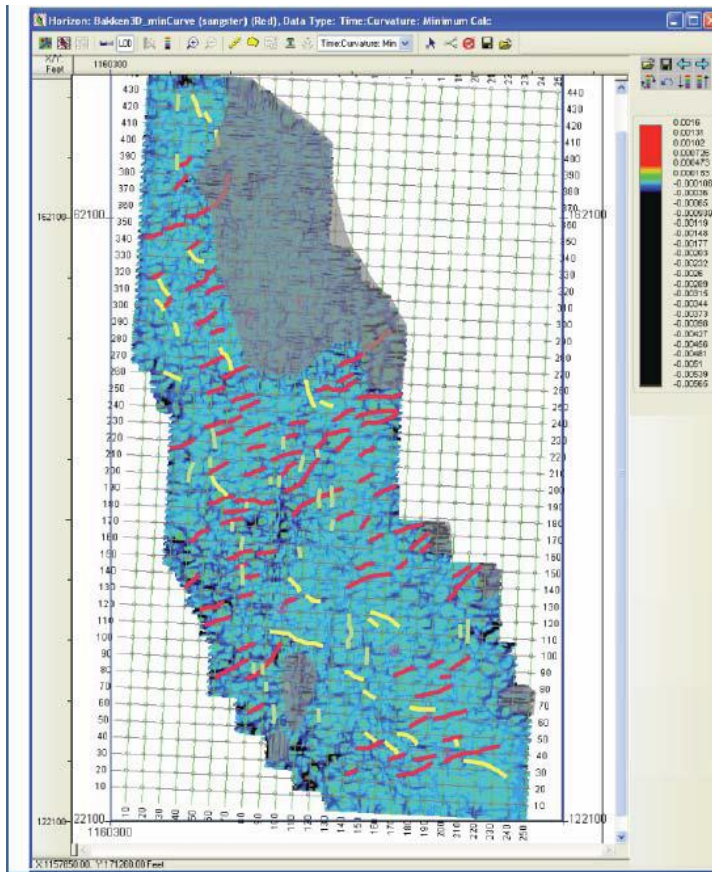
Figure 33. Hinge perpendicular or oblique (purple) and hinge parallel (blue) fracture distribution by lithology at Clarks Fork Canyon, Wyoming location. Hinge parallel fractures are more abundant in sandstone layers. Shale layers have a few axis perpendicular fractures.

**Stress-related regional fractures:** A regional fracture system oriented in both NE-SW and NW-SE directions is evident from the field data, and suggests right-lateral strike slip movement along major lineament trends (Angster, 2010). Vertical fractures paralleling the maximum horizontal stress are thought to be the open fracture direction. Oriented cores in the Bakken producing area of the Elkhorn Ranch and Roosevelt field areas on the Billings nose suggest that the maximum horizontal stress ( $\sigma^1$ ) is N45E (Cramer, 1991). Multi-well interference testing in the Billings nose indicates restricted hydraulic communication exists between wells off the N45E trend. Hydraulic fractures in Sanish Field also follow this NE-SW direction based on micro-seismic data (Whiting, 2010). The fracture orientation appears remain fairly constant through various horizons. Most operators orient their wells to cross this fracture direction: NS or NW-SE.

The Bicentennial 3D seismic data illustrates both aspects of regional and local structural controls on fracture trends and ultimately, well productivity. These data show a subtle structure at the Bakken-Three Forks level (Figure 34A). The minimum curvature attribute was found to be the most definitive in identifying potential fracture trends and shows a strong NE-SW trend direction as well as minor N and NW-SE trends (Figure 34B). The north trending fractures follow the hinge parallel direction. The NE-SW and NW-SE trends parallel the orthogonal regional trend, but also the hinge oblique directions as well. The dominant NE-SW trend is thus probably a combination of regional and local fracture systems (Figure 34B). Figure 35 shows that the horizontal well azimuths for highly productive wells are oriented NW-SE, perpendicular to the NE-SW fracture trend.



A.



B.

Figure 34. A. Bicentennial 3D seismic cube from north nose of the Billings Anticline showing subtle structure on top Bakken horizon (isochron map lower right of figure). B. Map of minimum curvature trends in Bakken structure. Red is hinge perpendicular or oblique and yellow is hinge parallel fracture trends. Rose diagram calculated from seismic attribute map, and shows

dominant NE-SW fracture trend that is interpreted to represent the combined regional and local structural trends.

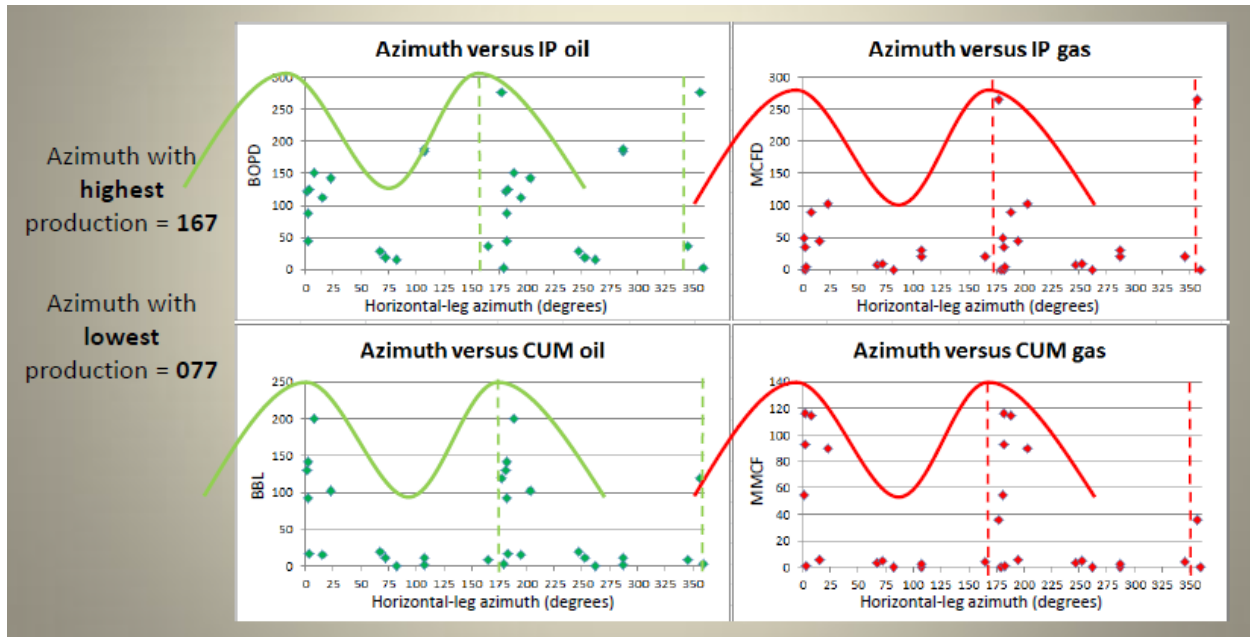


Figure 35. Horizontal well azimuths for wells drilled off structure in the Bicentennial area. Best production is from wells oriented perpendicular to the NE-SW regional trend.

To further test the local plus regional structural controls on fractures and productivity, eight wells were identified on the western flank of the Bicentennial structure (Figure 36). These wells show a range of productivity related to their orientation to the NS and NE-SW fracture trends as determined by the minimum curvature attribute (Figure 37). Figure 37 demonstrates that those wells oriented at a high angle to the NS and NE-SW fracture trends have the highest productivity, with most wells producing at greater than 100,000 barrels of initial and cumulative production (Figure 38).

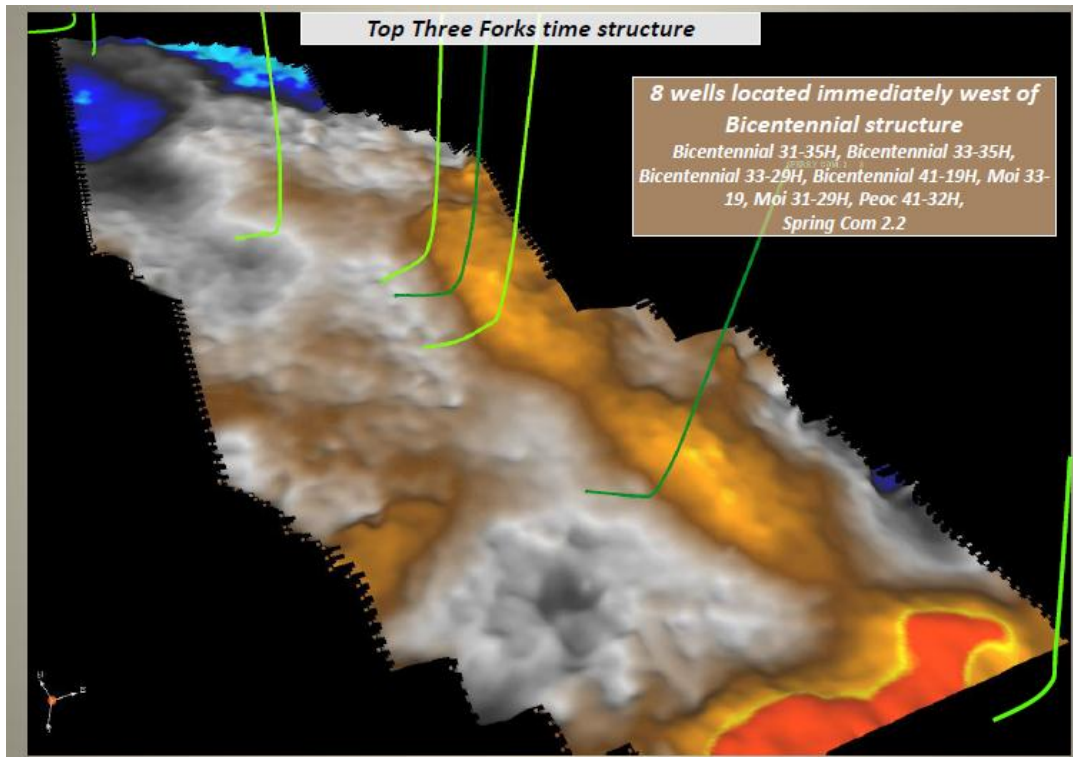


Figure 36. Time structure map on the Bakken-Three Forks (warm colors are structural highs). Locations of eight wells on flank of structure are shown.

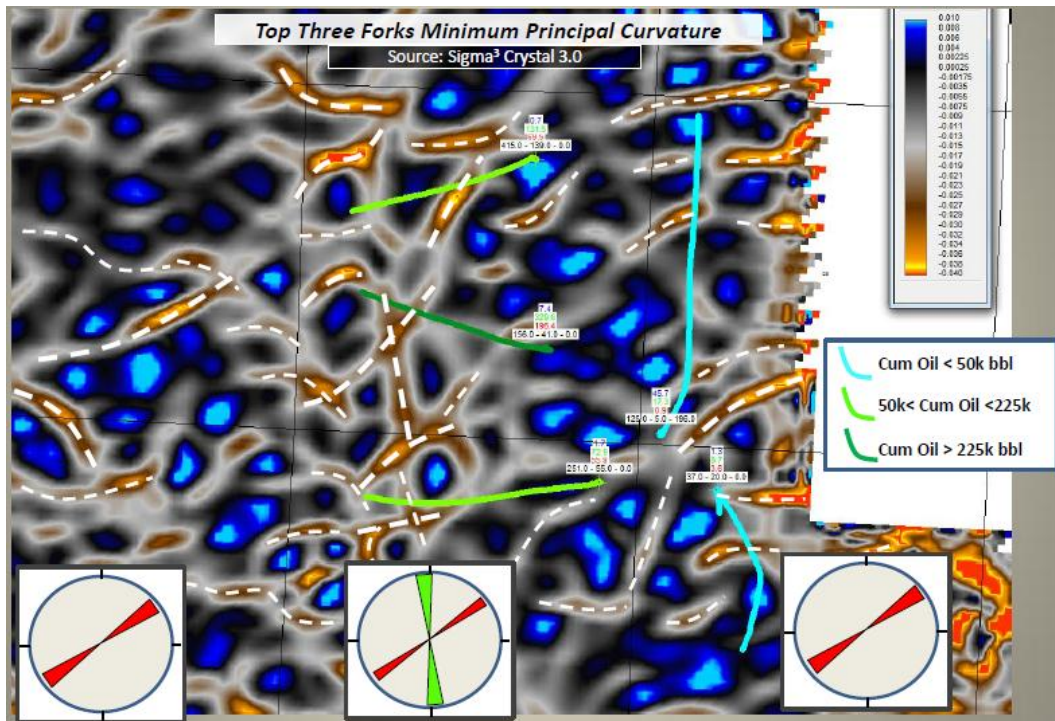


Figure 37. Minimum attribute map showing hinge parallel (NS) and hinge oblique (NE-SW) fractures.

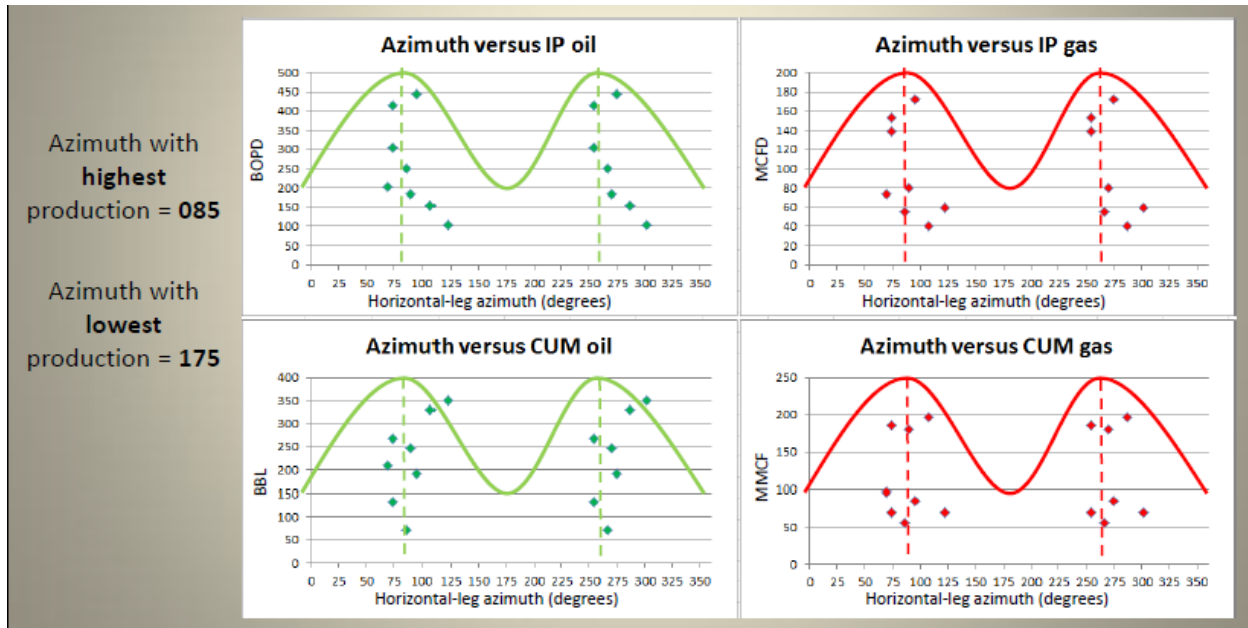


Figure 38. Horizontal well azimuths for wells drilled on structure in the Bicentennial area. Best production is from wells oriented at a high angle to the NS and NE-SW regional trends.

**Expulsion fractures associated with overpressure:** Micro-fracturing due to overpressuring of enclosed pore fluids suggests that a large increase in pore pressure may be sufficient to overcome the capillary pressure or even exceed the mechanical strength of the rock and induce micro-cracking. These types of micro-fractures are restricted to deeply buried, compacted, low permeability rocks. With thermal maturity, organic matter generates liquid or gaseous low molecular weight compounds. The mechanical strength of a rock is exceeded and fracturing occurs if the internal fluid pressure in a rock or in local pressure centers inside the pores is greater than a factor of 1.42 to 2.4 over the hydrostatic pressure in immediate surroundings. Pressures that exceed normal hydrostatic and even lithostatic pressure are possible whenever massive generation of gas and oil from kerogen takes place.

Horizontal and sub-horizontal expulsion fractures have been reported in the Bakken shales in clay- and organic-rich intervals (Carlisle et al., 1992; Pitman et al., 2001; Vernik, 1994; Hill, 2010). The fractures created by hydrocarbon overpressures are dominantly horizontal and are rarely mineralized. Early CO<sub>2</sub> driven expulsion of indigenous bitumen may also occur. Copious amounts of CO<sub>2</sub> are generated at immature ranks from highly organic-rich source beds. Water present in the shales chemically reacts with kerogen. Hydrogen from the water hydrogenates the kerogen, and oxygen from the water is given off as CO<sub>2</sub>. C<sub>2</sub> to C<sub>4</sub> gases are also generated in small amounts. The sum total of these reactions is a volume expansive reaction (Price, 1999). Strong mechanical strength anisotropy of kerogen-rich shales caused by bedding-parallel alignment of kerogen micro-layers and clay (illite) platelets probably facilitates this process (Vernik, 1994). Laboratory measurements of ultrasonic velocity and anisotropy in Bakken shales suggest that there are extensive, bedding-parallel microcracks. Fracture toughness of bedding-parallel cracks has been shown to be 30 percent lower than that of bedding-perpendicular ones in both kerogen rich and poor shales. SEM work suggests that overlapping illite platelets are sites for initial flaws. Penny shaped microcracks develop between two dissimilar minerals and micro-

cracks originate in kerogen-illite interfaces because of extreme low-fracture toughness of organic material (Vernik, 1994). QEMSCAN analysis supports this interpretation (Figure 39). Significant laminar micropores are evident in backscatter SEM images from Bakken shale samples.

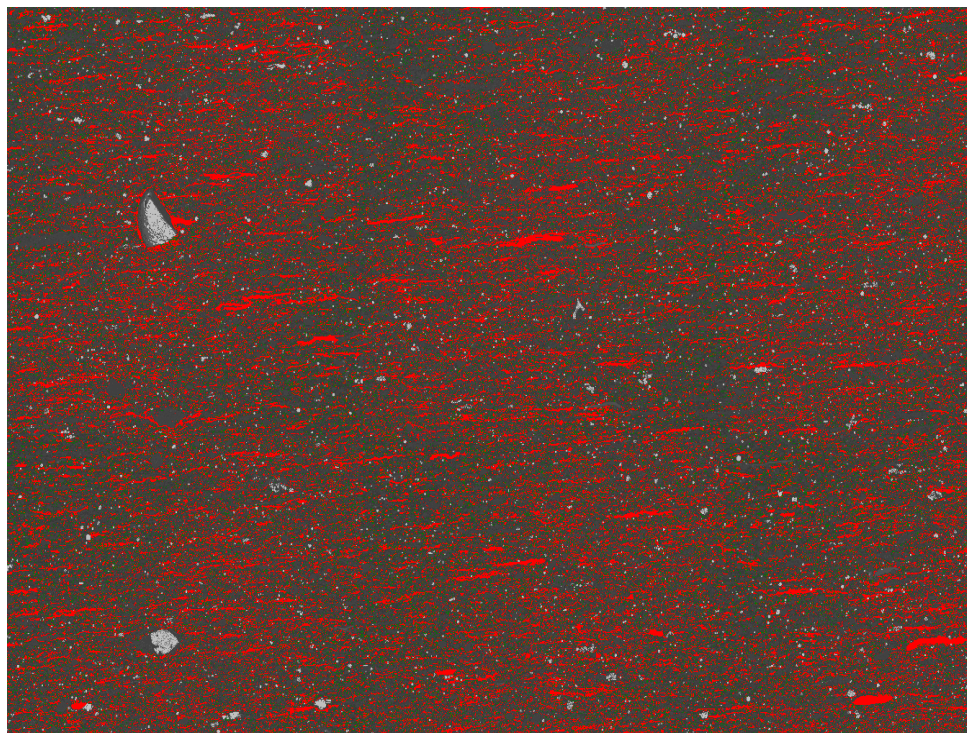


Figure 39. QEMSCAN backscatter image of Bakken shale showing mineral (black) and porosity + organic matter (red). Sample is mature and organic matter probably dominantly occupies pore space. Pore space is interpreted to be laminar microfractures created by expulsion of maturing hydrocarbons.

In summary:

1. Regional fractures form an orthogonal set with a dominant NE-SW trend parallel to  $\sigma^1$ , and a less prominent NW-SE trend. Many horizontal wells are drilled perpendicular to the  $\sigma^1$  direction to intersect these fractures.
2. Local structures formed by basement tectonics or salt dissolution form both hinge parallel and hinge oblique fractures that may overprint and dominate the local fracture signature.
3. Horizontal micro-fractures formed by oil expulsion in the Bakken shales, and connected and opened by hydro-fracturing provide permeability pathways for oil flow into wells that have hydro-fractured Middle Bakken facies.

### **INTEGRATED GEO-MODEL AT ELM COULEE FIELD**

The 3-D model constructed in Elm Coulee Field (Figure 40) was completed using the Schlumberger Petrel software version 2010.1. The support of the regional Schlumberger office in Greenwood Village, Colorado greatly aided in building the geo-model. The reservoir model was completed using a data subset of the total field area (Figure 41). The reason for this was to re-

duce the size of the model to help with computational processing speed. The area selected incorporated two cored wells, and has features displaying interpreted matrix and fracture properties.

Using formation and facies well tops of the Lodgepole, Bakken, and Three Forks formations, structure maps were built in Geographix petroleum geology software. The contoured surfaces were converted into grid layers that were used as three dimensional surfaces and imported into the Petrel static model (Figure 42).

Once the structure and thickness of the model are imported, the model was populated with cells forming a geo-cellular grid. The cells were then populated with lithological, and reservoir properties derived from core and petrophysical analyses. The grid cell size is chosen for its ability to show important geologic properties and also allows a reasonable time for computer simulation runs. The grid size chosen for this project is 100x100 ft. This grid cell size allowed for the capture of hydraulic fracture spacing intervals that can be modeled in a producing Bakken well. The geo-cellular grid was oriented in the maximum principal stress direction N60E, to best capture the fractures in the study area which are perpendicular to the majority of the drilled horizontal wells.

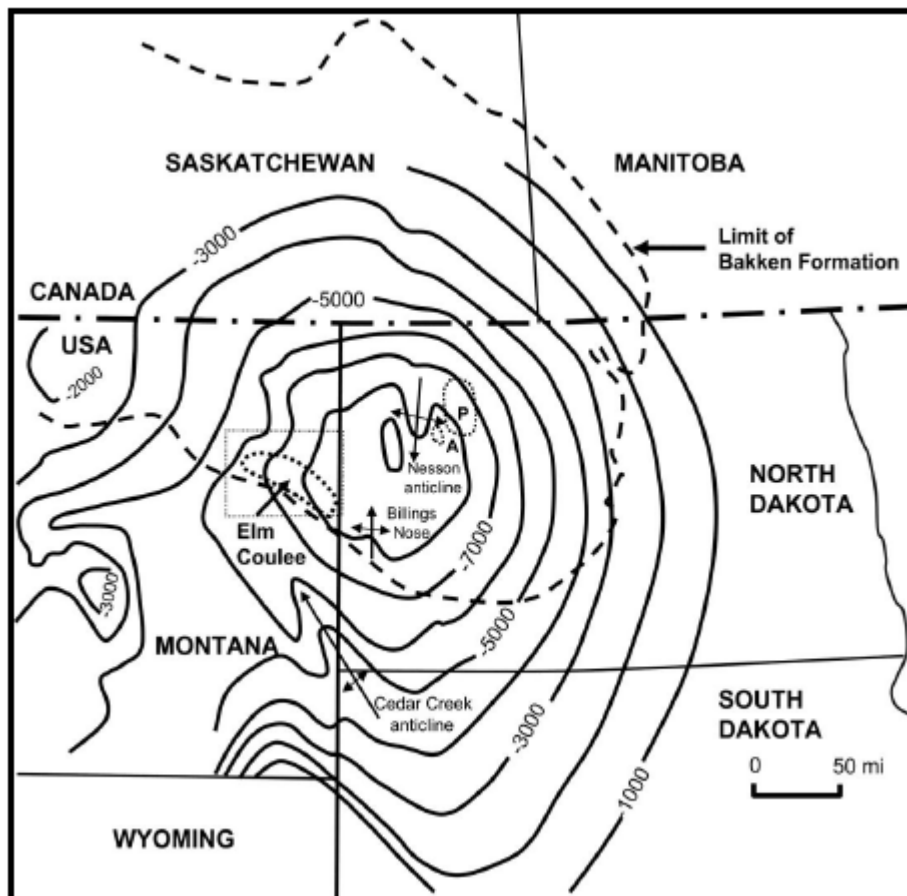


Figure 40. Location of Elm Coulee Field. Structure contours on base Mississippian Lodgepole Formation (from Sonnenberg and Pramudito, 2009).

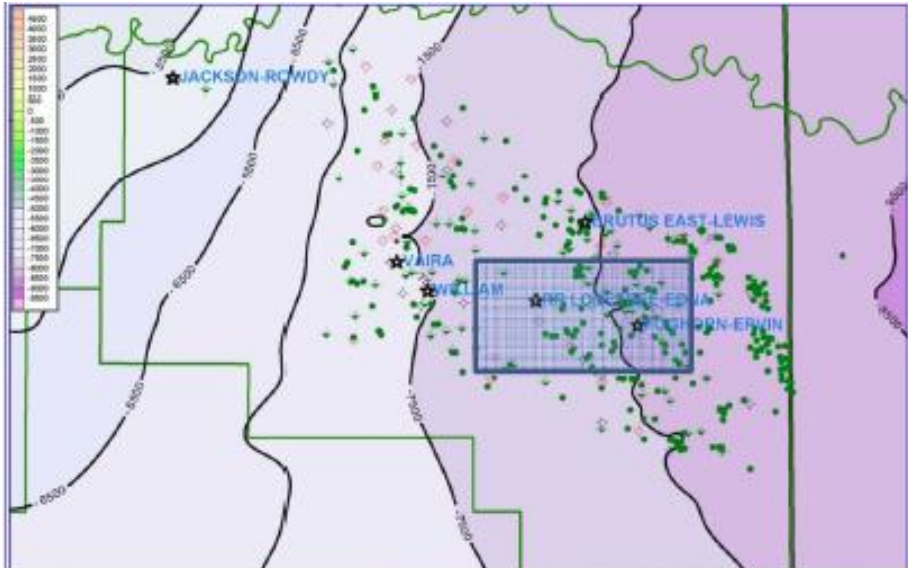


Figure 41. Box outlines area of Petrel model and shows locations of wells used to distribute petrophysical properties.

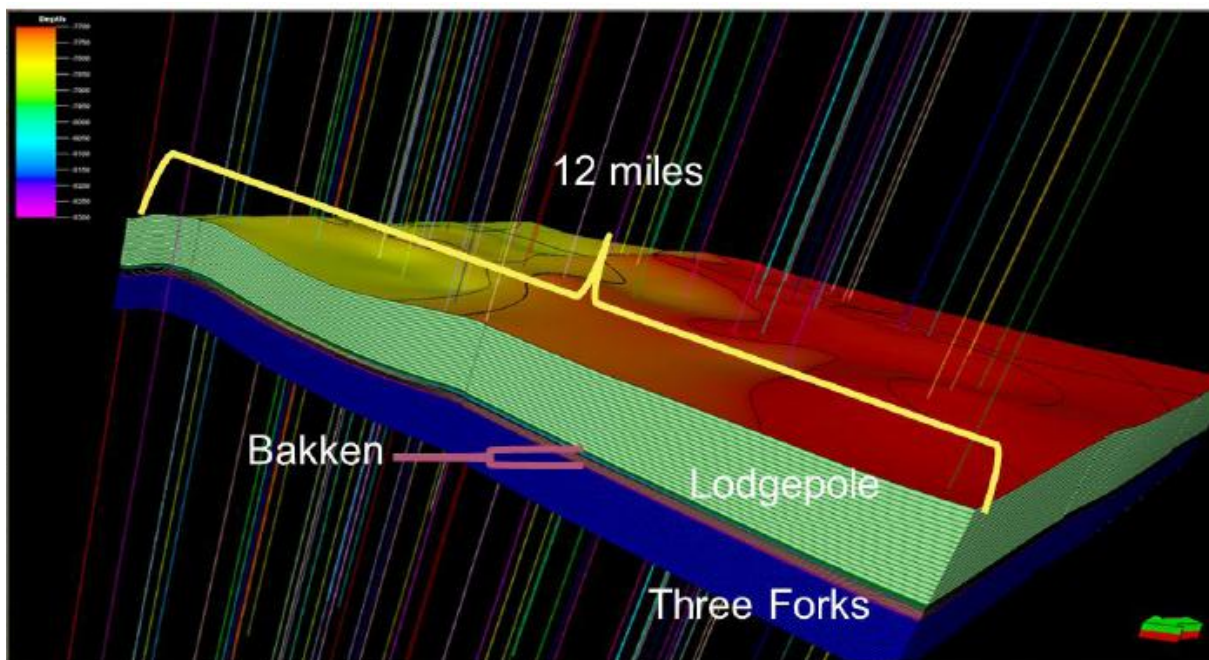


Figure 42. Petrel structural model and geo-cellular grid (grid size 100x100 ft.). The mapped horizons are Three Forks (blue), Bakken (brown and dark green), and Lodgepole (light green) formations.

The Middle Bakken lithofacies present at Elm Coulee are the Middle Bakken A, B, C, E, and F, with B and C making up the bulk of the facies present (Alexandre, 2011) (Figure 43). Over most of the field area the Three Forks underlies the Middle Bakken, except for the wedge edge of the Lower Bakken shale which is present on the northern margin of the field. Within the Middle Bakken, the presence of dolomite is most common within the B and C facies (Figure 44), and is the highest quality reservoir. Figure 45 shows an isopach map of average porosity for the Mid-

the Bakken with well spots showing production greater than 250,000 barrels. These best wells are located in the higher porosity areas containing the more dolomitized facies.

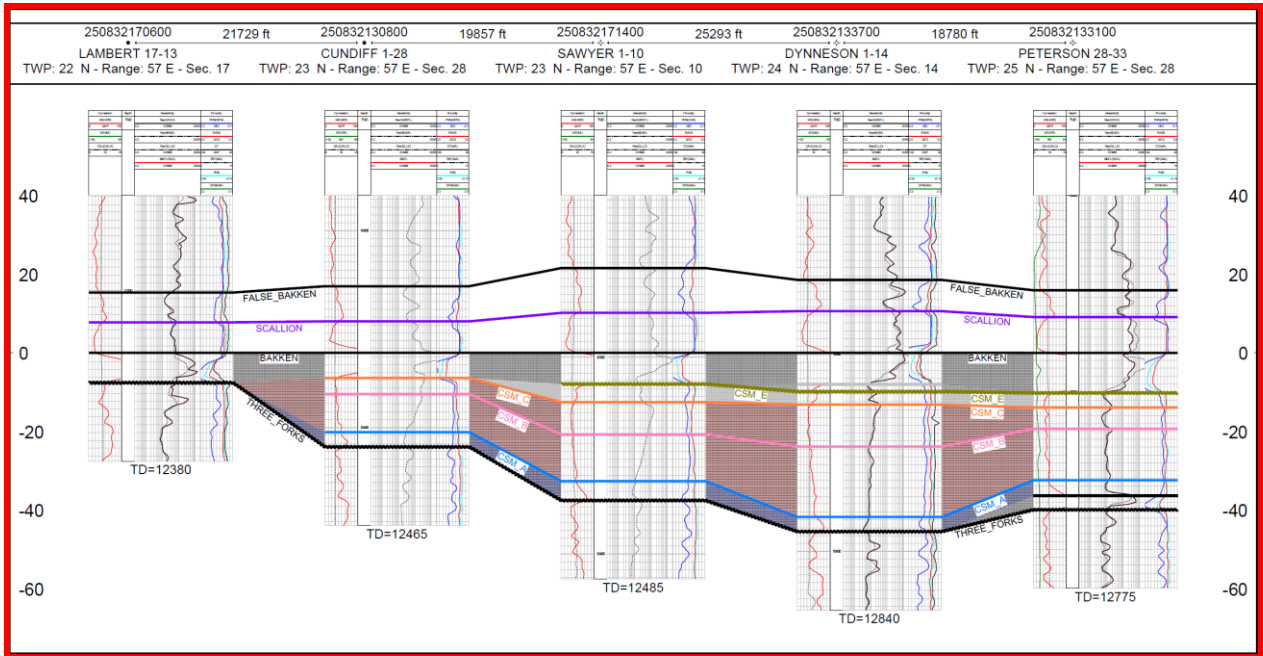
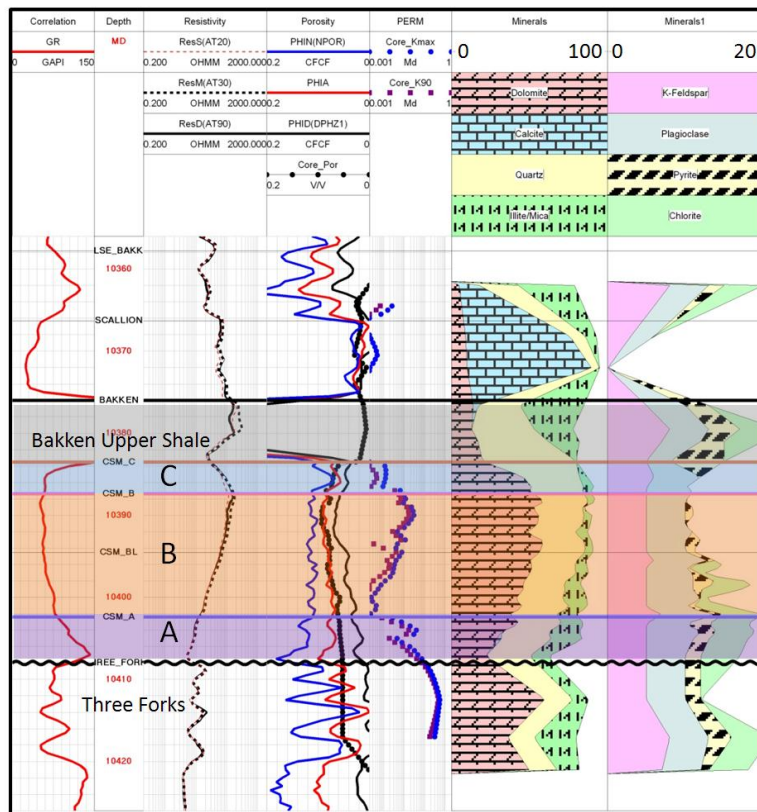


Figure 43. SW (left)-NE (right) stratigraphic cross section across Elm Coulee field.

Elm Coulee Middle Bakken Reservoir  
Lone Tree Edna 1-13



Facies C :  
Rhythmic mm-cm  
laminated silty dolostone  
Average Porosity: 7%



B – Burrowed and  
bioturbated silty dolostone.  
Contains abundant clay  
rich, compacted  
helminthopsis and  
scalarituba burrows  
Average Porosity: 6.5%



A – Brachiopod-rich silty  
dolostone. Bioturbated in  
some areas. Contains  
crinoids and echinoderms  
fragments  
Average Porosity: 4.5%

Figure 44. Lonetree Edna well gamma ray, and core porosity, and permeability, and XRD analyses. These analyses show good porosity and permeability corresponding to areas with high amounts of dolomite, and low amounts of calcite and clay. Core photos illustrate most key lithofacies A, B, and C.

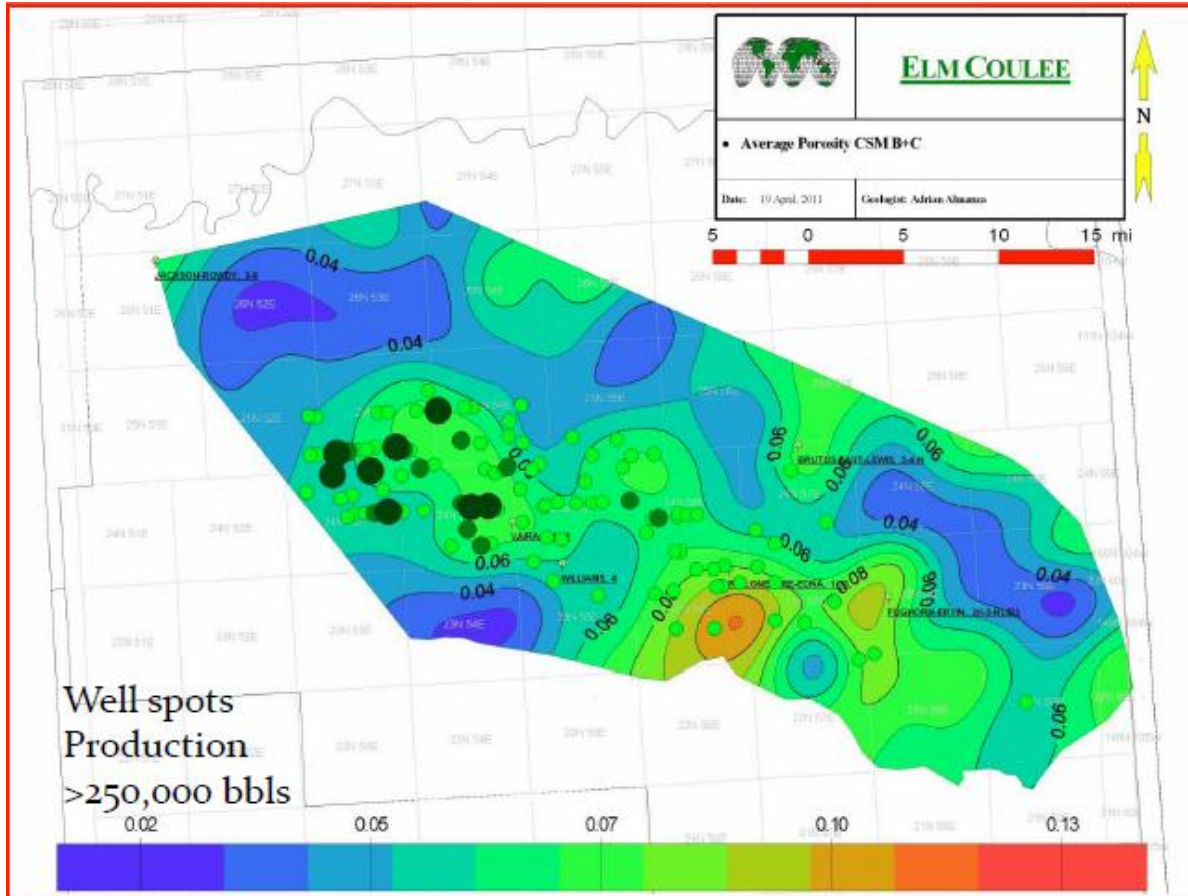


Figure 45. Isopach of Elm Coulee average porosity calculated from density porosity and neutron porosity logs. Well spots indicate cumulative production greater than 250,000 barrels.

Data from the well logs and core were used to calibrate petrophysical properties (Figure 46). These properties were then used to calculate average porosity (PHIA) and permeability (Perm) for the other wells used in this study. The permeability and porosity were converted into digital well logs that could be imported into Petrel software. The wells used were selected on their availability of digital logs, and the ability to calculate reservoir properties. Wells needed to have resistivity, porosity and gamma ray well log curves. A deterministic modeling method was used to construct the model. The density of the well logs and the ability to upscale the well-log data was a primary reason for using this method. This type of modeling is faster to run and gives a single estimated result. The averaging method used for porosity was an arithmetic mean which is recommended for this attribute. The preferred averaging method for the permeability was a harmonic mean averaging which works well for attributes with log normal distribution. The algorithm for distributing all the properties is a Gaussian Random Function Simulation developed by Petrel. Figure 47 shows the porosity and permeability volumes generated for the Middle Bakken reservoir matrix.

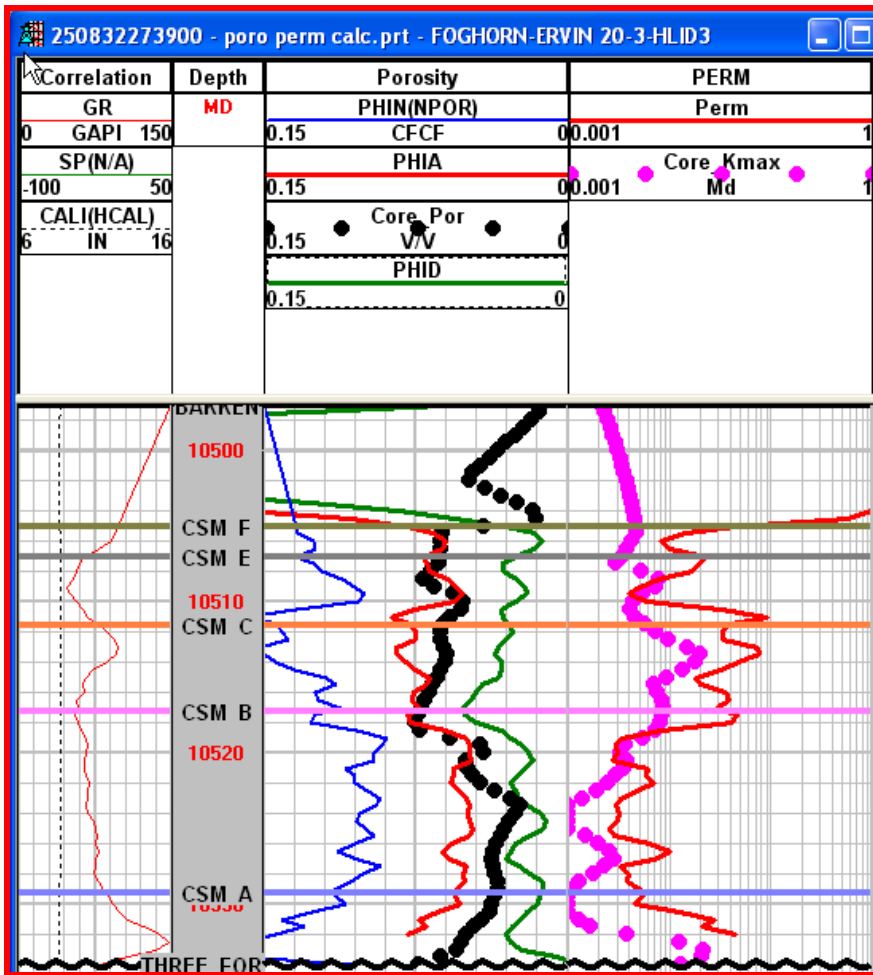
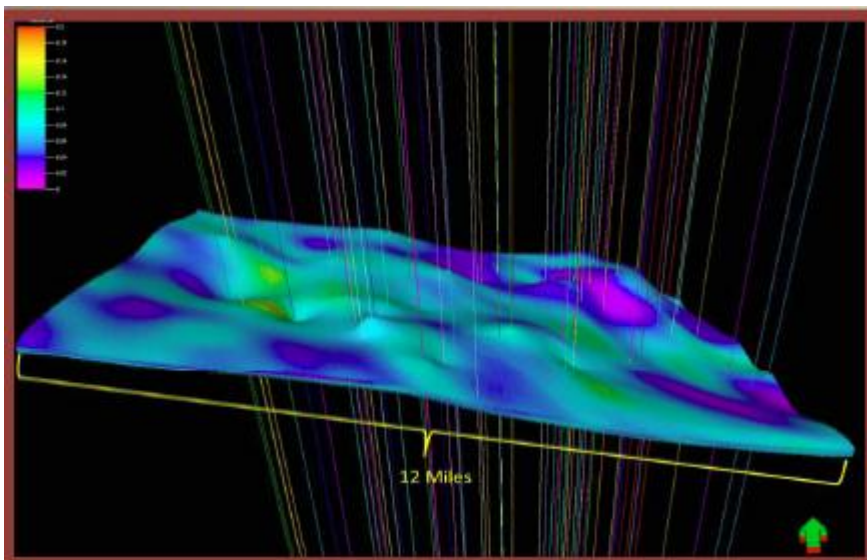
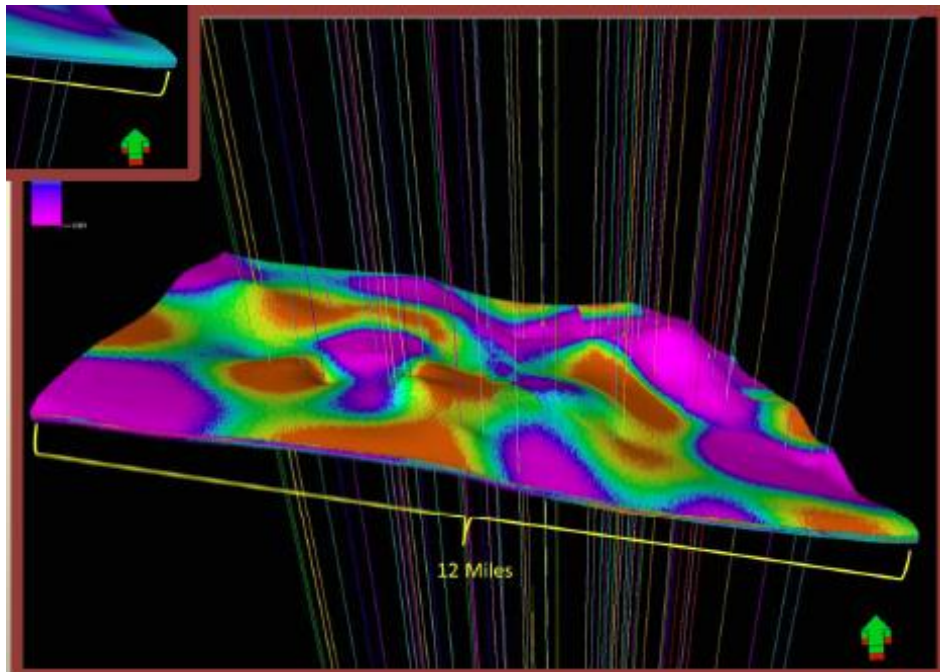


Figure 46. Measured porosity and permeability from Foghorn-Ervin well core.



A.



B.

Figure 47. A. Middle Bakken porosity map, minimum = 0% (purple), and maximum = 8% (yellow). B. Middle Bakken permeability, minimum = 0.001 mD (purple), and maximum = 0.1 mD (red).

Fractures may contribute to production, and two fracture features were considered, the regional fracture patterns seen in seismic and micro-seismic, and the fracture swarms inferred from the variation in production data across the field. The regional fracture fabric is oriented in two directions. The major fracture set is oriented to the northeast in the maximum principal stress direction N60E and the orthogonal fracture orientation is N150E. The fracture spacing (Figure 48) is based on observations from seismic (Angster, 2010), micro-seismic data taken by Inerplus Resources, and the distribution and trends of high well productivity (Almanza, 2011). The regional fracture trend oriented in the direction of maximum principal stress have a spacing of about 1,250 feet as was observed in both the micro-seismic and the Bicentennial seismic data. The orthogonal regional fracture direction has a spacing of approximately 2,500 feet (Figure 48). The fracture swarm trends (Figure 48) are spaced approximately 4.75 miles or 25,000 feet apart. This spacing is based on the orientation and distribution of the high productivity wells. Figure 49 shows a map of initial production with no bias imposed, and Figure 50 shows the map contoured with a moderate N60E bias applied. Figure 51 shows the cumulative production values combined with the interpreted fracture swarms, and an isopach map of porosity greater than 6%. This shows a strong correlation between high porosity, inferred fracture swarms, and cumulative production.

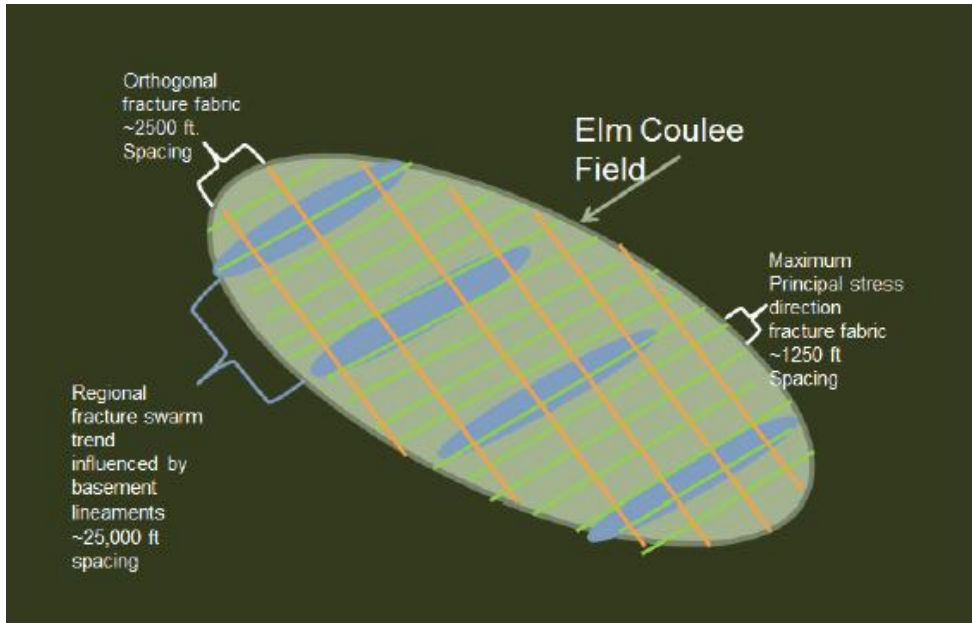


Figure 48. Fracture model developed for Elm Coulee.

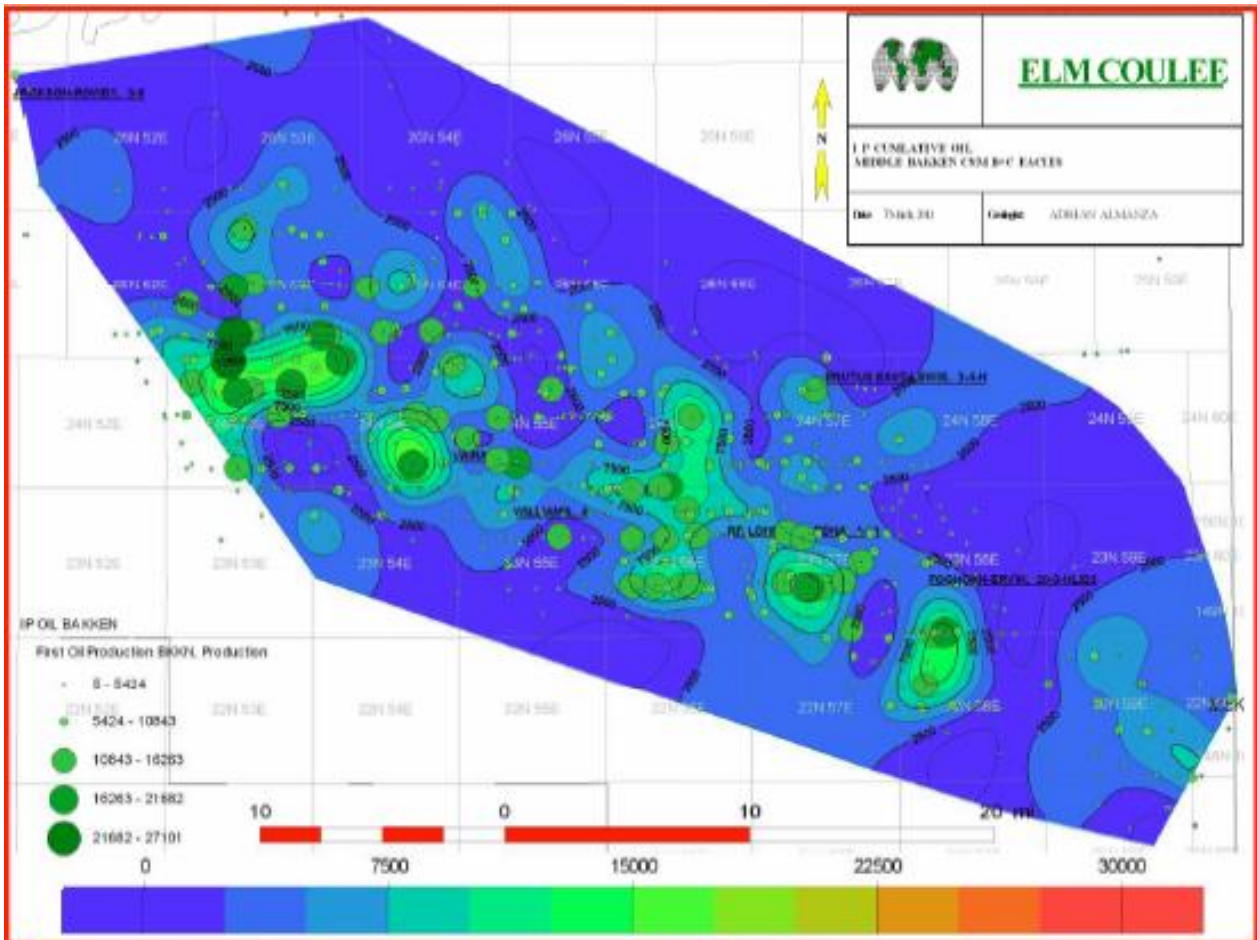


Figure 49. Contour map of first year cumulative production at Elm Coulee.

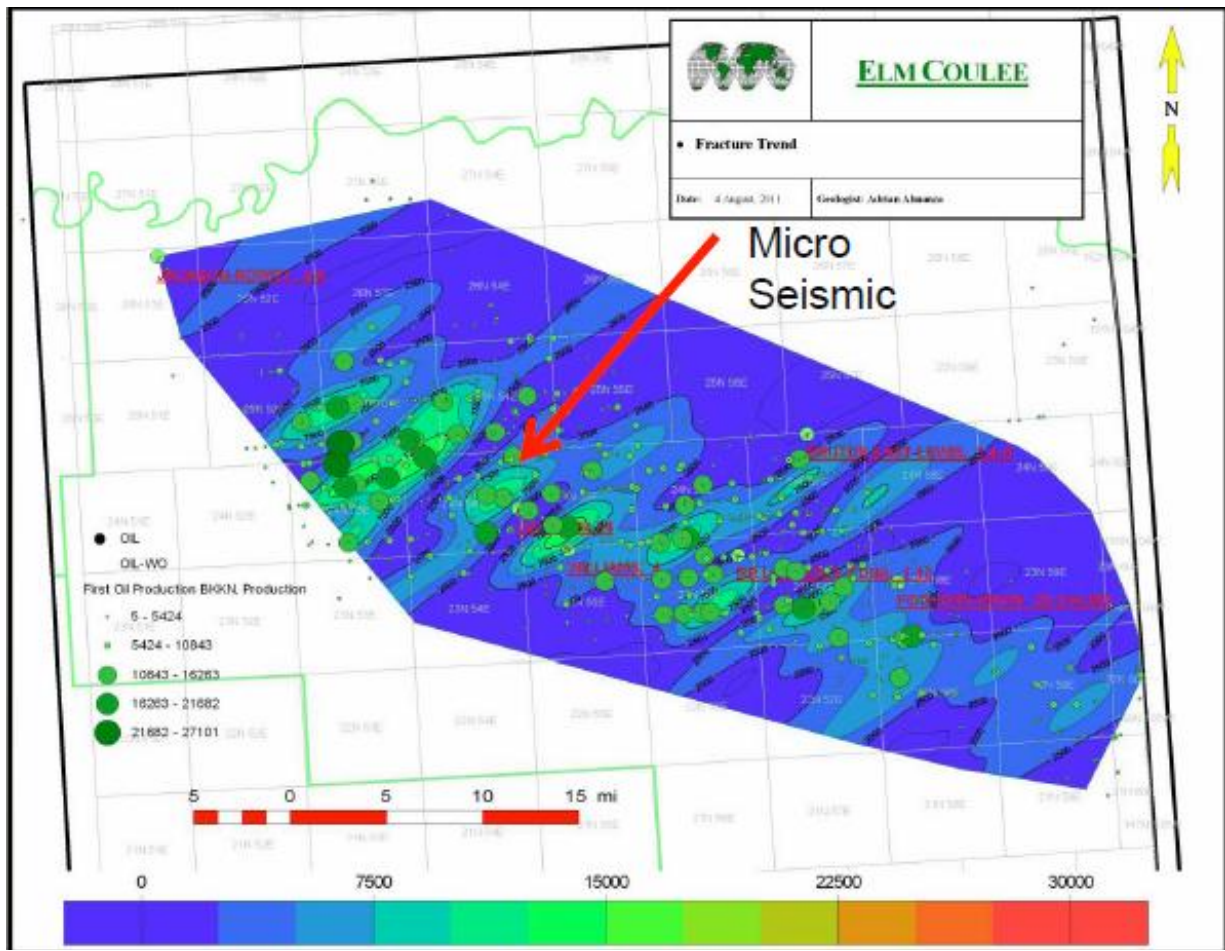


Figure 50. Contour map of first year cumulative production with moderate N60E bias trend imposed on production values.

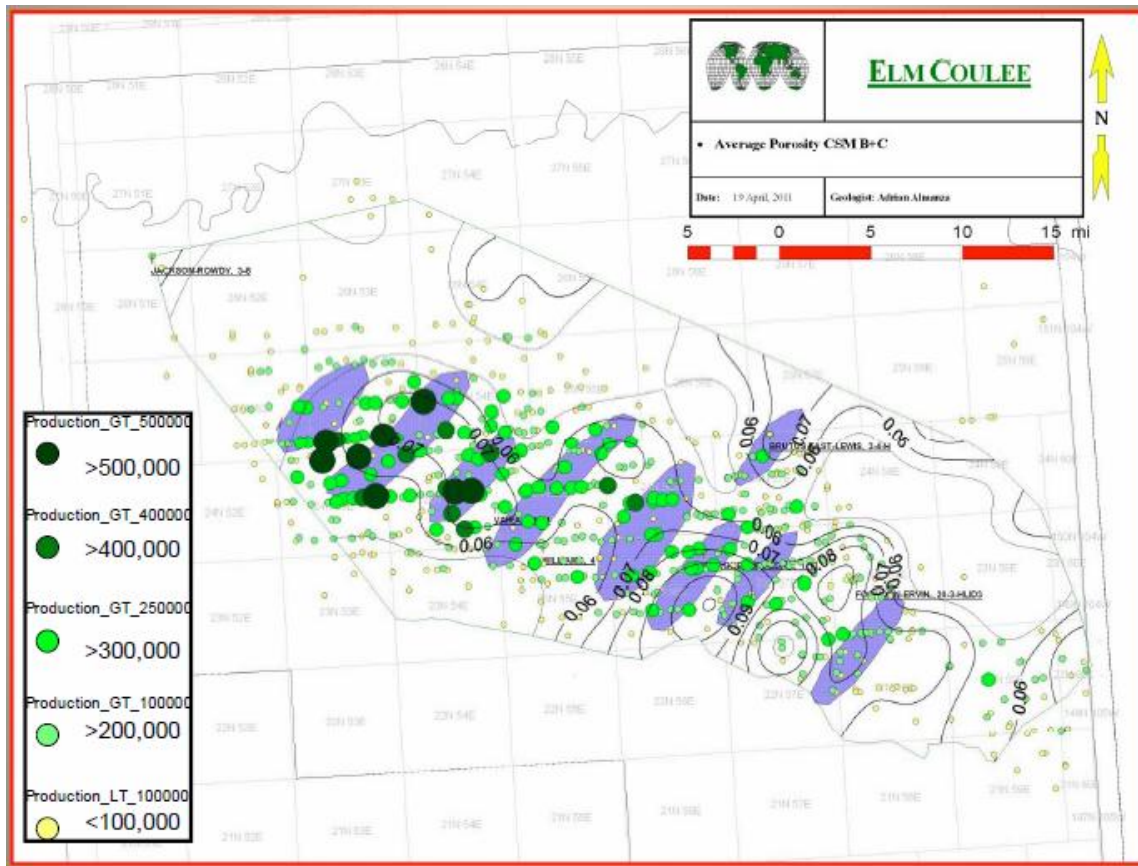


Figure 51. Cumulative production superimposed on porosity greater than 6% and fracture swarm locations.

The Petrel fracture model was then constructed using the model illustrated in Figure 48. Using the grid unit area of 100 by 100 ft, the ratio of 0.08 fractures per unit area (F/A) was used for the principal stress direction, and 0.04 F/A was used for the orthogonal fracture orientation. This ratio resulted in a fracture being placed every 1,250 ft in the maximum principal stress direction, and every 2,500 ft in the perpendicular orthogonal direction. The next step was to relate the localized fracture pattern to the initial production trends allowing for the most intense fracture contributions to come from the identified fracture swarm fairways. To accomplish this, first year cumulative production data was contoured and made into a surface, and then normalized. Localized fracture models were made for the two fracture directions displaying both observed spacing and lengths. The two localized fracture models were then multiplied by the normalized surface. The normalized surface had a high of 0.08 F/A in the northeast direction, and high of 0.04 F/A in the northwest direction respecting the localized fracture intensity patterns. The final result is a fracture model that has both the maximum principal stress direction fractures, and the orthogonal fractures that varied in fracture intensity according to the regional fracture model. The model is an interpreted fracture model that is related to production at Elm Coulee (Figure 52).

The fracture model and the matrix model were combined to construct a dual porosity model (Figure 53). **This Petrel dual porosity model, as well as copies of Almanza, 2011 are available as digital files that can be obtained from Colorado School of Mines, by contacting Dr. Sarg at [jsarg@mines.edu](mailto:jsarg@mines.edu).**

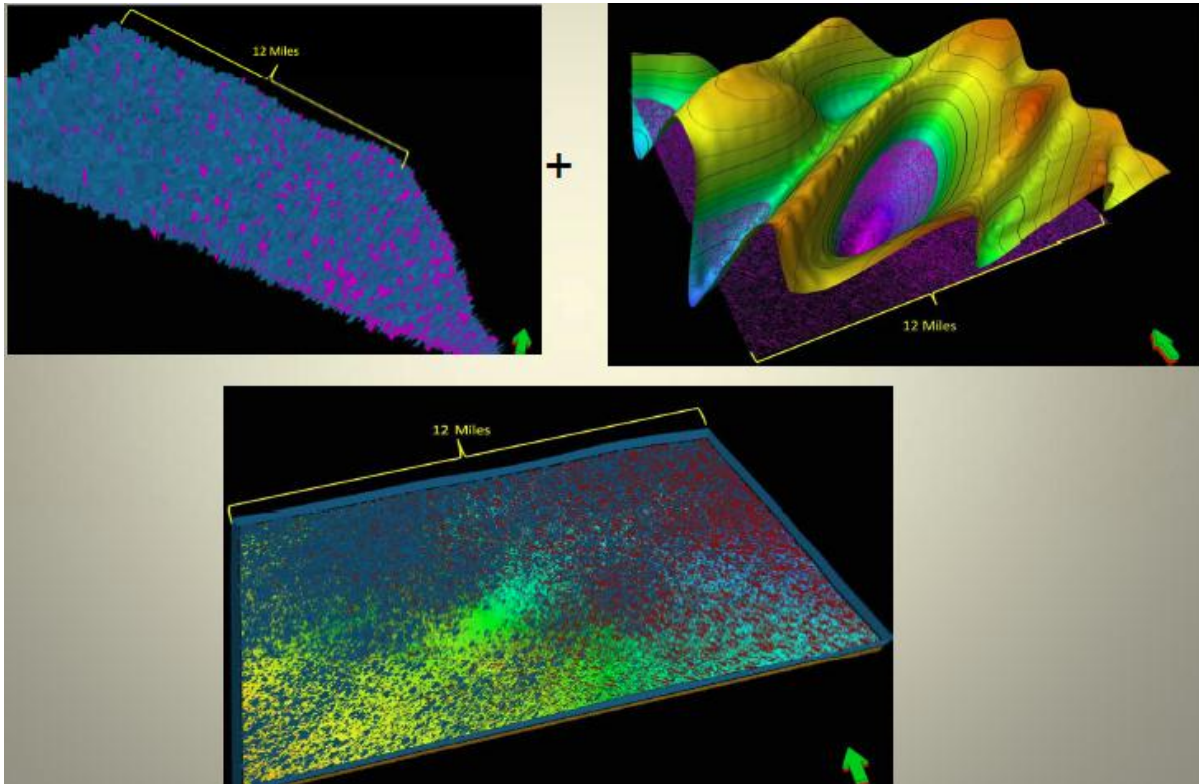


Figure 52. Petrel fracture model. Upper left displays the dominant northeast regional trend represented by blue polygons, and the orthogonal northwest fracture set represented by purple polygons. Upper right shows the regional fracture trends with first year production data contoured over them (contour interval 2,000 barrels of oil, orange is 18,000 barrels and the blue is 4,000 barrels of oil). Lower center shows an oblique view highlighting the fracture variability in the fracture model (blue polygons are NE fractures and red polygons are NW fractures).

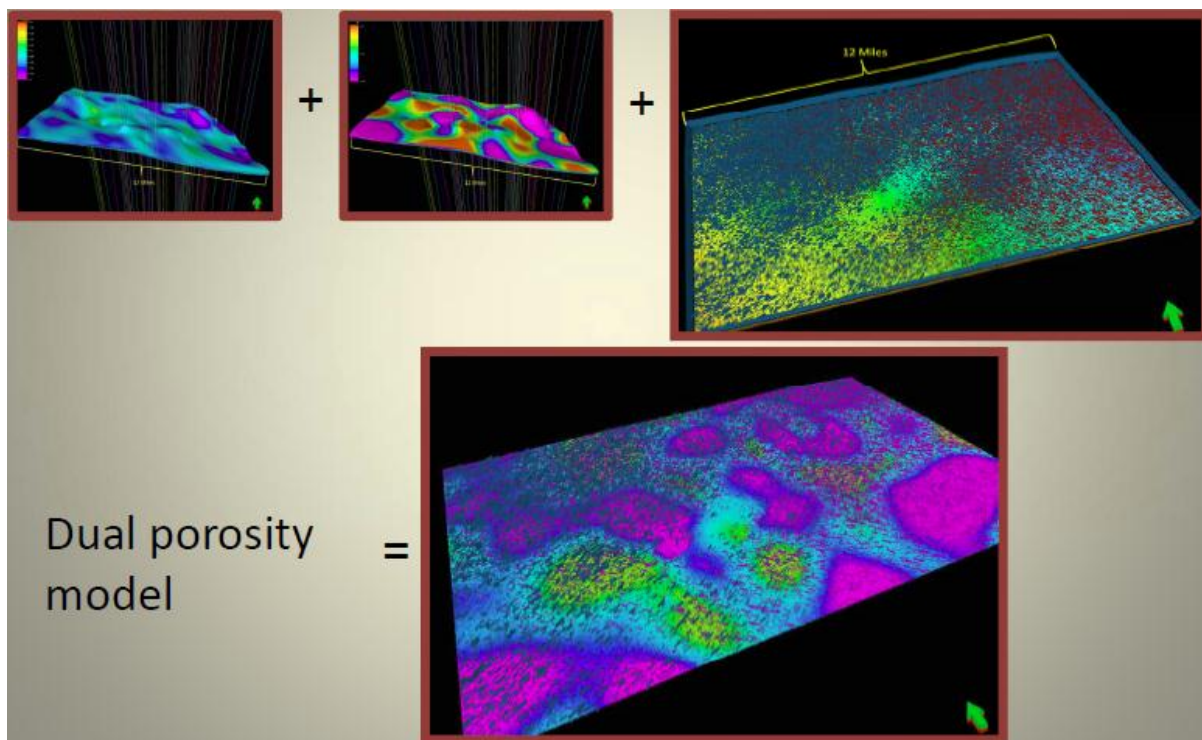


Figure 53. Matrix porosity/permeability model plus fracture model merged into dual porosity model.

In summary for the Elm Coulee geo-model:

1. Dolomitization played a key role in creating higher quality reservoir porosity and permeability.
2. High well productivity is located where fractures are present and are combined with favorable matrix properties.
3. First year cumulative production was the key factor in locating areas of high well productivity and deriving a fracture swarm distribution.
4. A dual porosity model was constructed using matrix properties and regional fracture trends enhanced with inferred fracture swarm distribution.

### **BAKKEN EXPLORATION MODEL**

Parameters and criteria have been developed to identify areas where new traps may be found, and where enhanced productivity of Bakken oil is possible. The criteria are grouped into four categories – (1) source and maturation, (2) reservoir quality of matrix, (3) natural fractures, and (4) trap and seal. This summary focuses on the Bakken Formation, but the following conclusions are applicable to the underlying Three Forks Formation.

The organic-rich Bakken shales are world class hydrocarbon source rocks. Kerogen is comprised of Type I and II, and total organic carbon (TOC) averages 11% and ranges from 8-16% over much of the Williston basin in North Dakota, and can attain values into the mid-30%. The

Bakken shales are mature over much of the basin, and are still generating oil (Sonnenberg, 2011). Large fields (Elm Coulee, Sanish, Parshall) are located at the transition from mature to immature level of maturation. Volume increases during maturation by as much as 30% providing necessary overpressure to allow highly productive wells. Volume decrease at the transition to immature source rock is important to providing updip top and lateral seal. Oil migration from the Upper Bakken shale probably has been over short distances (km to 10's of km), and has been mainly into the underlying Middle Bakken. Much of the oil remains within the Bakken Petroleum System.

Reservoirs are present both in the Middle Bakken and the Upper Bakken Shale. Middle Bakken facies B, C, D, and E can all be reservoirs, if quartz-rich and dolomite-rich (D facies) or dolomitized (B, C, and E facies). Porosity averages 4-8%, permeability averages 0.01-0.001 mD or less. Matrix reservoir quality is enhanced by dolomitization. Porosity is intercrystalline and tends to be greater than 6%. Permeabilities may reach to 0.15 mD or greater. This is a determinant for highly productive wells (e.g., Elm Coulee, Parshall, and Sanish). The Upper Bakken Shale is siliceous, which increases brittleness and enhances hydro-fracturing potential. During oil generation, the volume increase causes overpressure (0.6 - 0.73 psi/ft pressure gradient) and horizontal micro-fractures in the shale enhance permeability. Both the Middle Bakken and Upper Bakken Shale contribute to production.

Regional fractures and faults form an orthogonal set with NE-SW (dominant and parallel to  $\sigma^1$ ) and NW-SE orientations. Many horizontal wells are drilled perpendicular to  $\sigma^1$  direction to intersect these fractures. Local structures formed by basement tectonics or salt dissolution form both hinge parallel and hinge oblique fractures that may overprint and dominate the local fracture signature. Horizontal fractures formed by oil expulsion in shale and perhaps along bedding plane lamination of Middle Bakken C and E facies provide permeability pathways enhancing production.

Although the Bakken is a basinwide resource play, large accumulations such as at Elm Coulee, Sanish, and Parshall fields do appear to have significant trap and seal components. Top seal is provided by the Lodgepole Formation, and where immature, the Upper Bakken Shale. Lateral seals can occur where there is a facies change to more impermeable rock. Traps include 1) hydrodynamic at mature to immature boundary (e.g., Parshall field, North Dakota); 2) stratigraphic pinch out of the Middle Bakken (e.g., Elm Coulee field, Montana); 3) porosity pinch out of Middle Bakken dolomitic facies (e.g., Elm Coulee field, Montana), and 4) lateral facies changes in Middle Bakken (e.g., View Field, Canada).

## CONCLUSIONS

The important results of this integrated study of the Bakken Petroleum System can be briefly summarized as: (1) dolomite is needed for good reservoir performance in the Middle Bakken; (2) regional and local fractures play a significant role in enhancing permeability and well production, and it is important to recognize both, because local fractures will dominate in on-structure locations; and (3) the organic-rich Bakken shale serves as both a source and reservoir rock.

Bakken reservoirs are characterized by -

- Middle Bakken facies B, C, D, and E can all be reservoirs, if quartz and dolomite-rich (facies D) or dolomitized (facies B, C, E).
- Porosity averages 4-8%, permeability averages 0.001-0.01 mD or less.
- Matrix reservoir quality is enhanced by dolomitization. Porosity is intercrystalline and tends to be greater than 6%. Permeability may reach to 0.15 mD or greater. This appears to be a determinant of high productive wells (e.g., Elm Coulee, Parshall, and Sanish fields).
- The Upper Bakken Shale is siliceous, increasing brittleness and enhancing fracturing potential.

Mechanical properties of the Bakken Formation indicate that –

- The Bakken shales have similar effective stress as the Middle Bakken suggesting that the shale will not contain induced fractures, and will contribute hydrocarbons from interconnected micro-fractures.
- Organic-rich shale impedance will increase with a reduction in porosity, and an increase in kerogen stiffness during the burial maturation process, and thus, maturation can be directly related to impedance.

Fractures play a critical role in enhancing permeability and production -

- Regional fractures form an orthogonal set with a dominant NE-SW trend parallel to  $\sigma^1$ , and a less prominent NW-SE trend. Many horizontal wells are drilled perpendicular to the  $\sigma^1$  direction to intersect these fractures.
- Local structures formed by basement tectonics or salt dissolution form both hinge parallel and hinge oblique fractures that may overprint and dominate the local fracture signature.
- Horizontal micro-fractures formed by oil expulsion in the Bakken shales, and connected and opened by hydro-fracturing provide permeability pathways for oil flow into wells that have hydro-fractured the Middle Bakken facies.

The construction of a Petrel geo-model at Elm Coulee used the results of the lithofacies, mineral, and fracture studies to develop modeling parameters -

- Dolomitization formed higher quality reservoir porosity and permeability.
- High well productivity is located where natural fractures are present (as revealed by drill stem tests and micro seismic data), and are combined with favorable matrix properties.
- First year cumulative production was the key factor in locating areas of high well productivity and deriving a fracture swarm distribution.
- A dual porosity model was constructed using matrix properties and regional fracture trends that were combined with the inferred fracture swarm distribution.

## REFERENCES

- Alexandre, C., 2011. Reservoir Characterization and Petrology of the Bakken Formation, Elm Coulee Field, Richland Montana, Colorado School of Mines Ms. Thesis, 175 p.
- Almanza, A., 2011, Petrophysical Analysis and GeoModel of the Bakken Formation, Elm Coulee Field, Richland County, Montana, Colorado School of Mines Ms. Thesis, 111p.
- Angster, S., 2010, Fracture Analysis of the Bakken Formation, Williston Basin: Field Studies in the Little Rocky Mountains, Big Snowy Mountains, MT, and Beartooth Mountains, WY, Colorado School of Mines Ms. Thesis, 67p.
- Carlisle, J., L. Druyff, M. Fryt, J. Artindale, and H. Von Der Dick, 1992, The Bakken Formation—An integrated geologic approach to horizontal drilling, *in* J. E. Schmoker, E. Coalson, and C. Brown, eds., Geologic studies relevant to horizontal drilling: Examples from western North America: Rocky Mountain Association of Geologists, p. 215-226.
- Cramer, D. D., 1986, Reservoir characteristics and stimulation techniques in the Bakken Formation and adjacent beds, Billings Nose area, Williston Basin, *in* S. Goolsby and M. W. Longman, eds., Proceedings from SPE Rocky Mountain Region Technical Meeting: Society of Petroleum Engineers, Paper no. 15166, p. 331-344.
- Cramer, D. D., 1991, Stimulation treatments in the Bakken Formation: Implications for horizontal completions, *in* W. B. Hansen, ed., Geology and horizontal drilling of the Bakken Formation: Montana Geological Society, p. 117-140.
- FEI Company, Oil & Gas. [http://intellecion.com.au/oil\\_gas.html](http://intellecion.com.au/oil_gas.html). Visited February 22, 2010.
- Havens, J., 2012, Mechanical Properties of the Bakken Formation; Colorado School of Mines Ms. Thesis, 111p.
- Hill, R., 2010, Bitumen Filled Fractures in the Bakken Formation and Implications for Gas Shale Systems: AAPG Search and Discovery Article #90108©2010 AAPG International Convention and Exhibition, Calgary, Alberta, Canada.
- Hoal, Karin, P. W.S.K. Botha, A. Forsyth, A.R. Butcher, 2007, Advanced Mineralogy Research: Mineral Characterization Using QEMSCAN Techniques, GSA Denver Annual Meeting, Paper 75-15, 1 p.
- Hoal, Karin, S.K. Appleby, J.G. Stammer, C. Palmer, 2009a, SEM-based Quantitative Mineralogical Analysis of Peridotite, Kimberlite, and Concentrate: Lithos, v. 112, Supplement 1, p. 41-46.
- Hoal, Karin, J.G. Stammer, S.K. Appleby, J. Botha, J.K. Ross, P.W. Botha, 2009b, Research in Quantitative Mineralogy: Examples from Diverse Applications: Minerals Engineering, v. 22, issue 4, p. 402-408

Kowalski, B. L., 2010, Quantitative Mineralogical Analysis of the Middle Bakken Member, Parshall Field, Mountrail County, North Dakota, Colorado School of Mines Ms. Thesis, 152p.

LeFever, J. A., C. D. Martiniuk, E. F. R. Dancsok, and D. F. Lund, 1991, Petroleum potential of the middle member, Bakken Formation, Williston basin, *in* Christopher, J. E. and F. Haidl, eds., Proceedings of the sixth international Williston basin symposium: Saskatchewan Geological Society, Special Publication 11, p. 74–94.

LeFever, J., 2005, Oil production from the Bakken Formation: A short history: North Dakota Geological Survey Newsletter, v. 32, no. 1, p. 1-6.

Lineback, J. A., and M. L. Davidson, 1982, The Williston basin – sediment-starved during the Early Mississippian, *in* J.E. Christopher and J. Kaldi, eds., Fourth International Williston Basin Symposium, Saskatchewan Geological Society Special Publication 6, p. 125-130.

Meissner, F. F., 1978, Petroleum geology of the Bakken Formation, Williston basin, North Dakota and Montana, *in* D. Rehrig, ed., The economic geology of the Williston basin: Proceedings of the Montana Geological Society, 24th Annual Conference, p. 207–227.

Murray, G. H., 1968, Quantitative fracture study - Sanish pool, McKenzie County, North Dakota: AAPG Bulletin, v. 52, no. 1, p. 57-65.

Narr, W., and R. C. Burruss, 1984, Origin of fractures in Little Knife Field, North Dakota: AAPG Bulletin, v. 68, no. 9, p. 1087-1100.

Nordeng, S., 2009, A brief history of oil production from the Bakken Formation in the Williston Basin: North Dakota Geological Survey Newsletter, v. 37, no. 1, p. 5-9.

Pitman, J. K., Price, L. C., and LeFever, J. A., 2001, Diagenesis and fracture development in the Bakken Formation, Williston Basin: Implications for reservoir quality in the middle member: U.S. Geological Survey Professional Paper 1653, 17 p.

Price, L. C., 1999, Origins and Characteristics of the Basin-Centered Continuous Reservoir Unconventional Oil-Resource Base of the Bakken Source System, Williston Basin (unpublished), paper available at: <http://www.undeerc.org/Price/>.

Simenson, A. L., 2010, Depositional Facies and Petrophysical Analysis of the Bakken Formation, Parshall Field, Mountrail County, North Dakota, Colorado School of Mines Ms. Thesis, 196p.

Smith, M. G., and M. Bustin, 1996, Lithofacies and paleoenvironments of the upper Devonian and lower Mississippian Bakken Formation, Williston Basin: Bulletin of Canadian Petroleum Geology, v. 44, no. 3, p. 495-507.

Sonnenberg, S. A., 2011, TOC and pyrolysis data for the Bakken shales, Williston basin, North Dakota and Montana, *in* North Dakota, Rocky Mountain Association of Geologists publication,

The Bakken-Three Forks Petroleum System in the Williston Basin, J. W. Robinson, J. A. LeFever, and S. B. Gasworth, eds., p. 308-331.

Sonnenberg, S. A., and A. Pramudito, 2009, Petroleum geology of the giant Elm Coulee Field, Williston Basin: AAPG Bulletin, v. 93, no. 9 (September 2009) p. 1127-1153.

Sonnenberg, S. A., J. Vickery, C. Theloy, and J. F. Sarg, , 2011, Middle Bakken Facies, Williston Basin, USA: A Key to Prolific Production: poster presentation AAPG Annual Meeting, Houston, TX.

Sonnenberg, S. A., J. A. LeFever, and R. Hill, 2011, Fracturing in the Bakken Petroleum System, Williston Basin, *in* North Dakota, Rocky Mountain Association of Geologists publication, The Bakken-Three Forks Petroleum System in the Williston Basin, J. W. Robinson, J. A. LeFever, and S. B. Gasworth, eds., p. 393-417.

Sturm, S. D. and E. Gomez, 2009, Role of Natural Fracturing in Production from the Bakken Formation, Williston Basin, North Dakota: AAPG Annual Convention and Exhibition. Denver, Colorado.

Vernik, L., 1994, Hydrocarbon – generation – induces microcracking of source rocks: Geophysics, v. 59, no. 4, p. 555-563.

Vernik, L., and Nur, A., 1992, Ultrasonic velocity and anisotropy of hydrocarbon source rocks, Geophysics, v. 52, p. 727–735.

Vickery, J., 2010, Lithofacies, Mineralogy, and Ichnology of the Bakken Formation (Mississippian and Devonian), Williston Basin, Montana and North Dakota, USA, Colorado School of Mines Ms. Thesis, 252p.

Webster, R. L., 1984, Petroleum source rocks and stratigraphy of the Bakken Formation in North Dakota *in* Woodward J., F. F. Meissner, J. L. Clayton, eds., Hydrocarbon source rocks of the greater Rocky Mountain region, Rocky Mountain Association of Geologists, p. 57 - 82.

## **BIBLIOGRAPHY**

Almanza, A., 2011, Petrophysical Analysis and GeoModel of the Bakken Formation, Elm Coulee Field, Richland County, Montana, Colorado School of Mines Ms. Thesis, 111p.

Angster, S., 2010, Fracture Analysis of the Bakken Formation, Williston Basin: Field Studies in the Little Rocky Mountains, Big Snowy Mountains, MT, and Beartooth Mountains, WY, Colorado School of Mines Ms. Thesis, 67p.

Havens, J., 2012, Mechanical Properties of the Bakken Formation, Colorado School of Mines Ms. Thesis, 111p.

Kowalski, B. L., 2010, Quantitative Mineralogical Analysis of the Middle Bakken Member, Parshall Field, Mountrail County, North Dakota, Colorado School of Mines Ms. Thesis, 152p.

Kowalski, B. L., and S. A. Sonnenberg, 2011, Mineralogic analysis of the Middle Bakken Member, Parshall field area, Mountrail County, North Dakota, *in* North Dakota, Rocky Mountain Association of Geologists publication, The Bakken-Three Forks Petroleum System in the Williston Basin, J. W. Robinson, J. A. LeFever, and S. B. Gasworth, eds., p. 102-126, .

Mba, K., 2010, Organic-rich Shale Maturity: Velocity and Impedance Analysis in the Bakken Shales, Colorado School of Mines Ms. Report.

Simenson, A. L., 2010, Depositional Facies and Petrophysical Analysis of the Bakken Formation, Parshall Field, Mountrail County, North Dakota, Colorado School of Mines Ms. Thesis, 196p.

Simenson, A. L., S. A. Sonnenberg, and R. M. Cluff , 2011, Depositional facies and petrophysical analysis of the Bakken Formation, Parshall field and surrounding area, Mountrail County, *in* North Dakota, Rocky Mountain Association of Geologists publication, The Bakken-Three Forks Petroleum System in the Williston Basin, J. W. Robinson, J. A. LeFever, and S. B. Gasworth, eds., p. 48-101.

Sonnenberg, S. A., 2011, TOC and pyrolysis data for the Bakken shales, Williston basin, North Dakota and Montana, *in* North Dakota, Rocky Mountain Association of Geologists publication, The Bakken-Three Forks Petroleum System in the Williston Basin, J. W. Robinson, J. A. LeFever, and S. B. Gasworth, eds., p. 308-331.

Sonnenberg, S. A., J. A. LeFever, and R. Hill, 2011, Fracturing in the Bakken Petroleum System, Williston Basin, *in* North Dakota, Rocky Mountain Association of Geologists publication, The Bakken-Three Forks Petroleum System in the Williston Basin, J. W. Robinson, J. A. LeFever, and S. B. Gasworth, eds., p. 393-417.

Stroud, J., 2010, Petroleum Potential of the Lower Lodgepole Formation, Colorado School of Mines Ms. Thesis.

Stroud, J., and S. A. Sonnenberg, 2011, The role of the Lower Lodgepole Formation in the Bakken Petroleum System, Billings Nose, North Dakota, *in* North Dakota, Rocky Mountain Association of Geologists publication, The Bakken-Three Forks Petroleum System in the Williston Basin, J. W. Robinson, J. A. LeFever, and S. B. Gasworth, eds., p. 332-364.

Vickery, J., 2010, Lithofacies, Mineralogy, and Ichnology of the Bakken Formation (Mississippian and Devonian), Williston Basin, Montana and North Dakota, USA, Colorado School of Mines Ms. Thesis, 252p.

## **National Energy Technology Laboratory**

626 Cochran's Mill Road  
P.O. Box 10940  
Pittsburgh, PA 15236-0940

3610 Collins Ferry Road  
P.O. Box 880  
Morgantown, WV 26507-0880

One West Third Street, Suite 1400  
Tulsa, OK 74103-3519

1450 Queen Avenue SW  
Albany, OR 97321-2198

2175 University Ave. South  
Suite 201  
Fairbanks, AK 99709

Visit the NETL website at:  
[www.netl.doe.gov](http://www.netl.doe.gov)

Customer Service:  
1-800-553-7681

